Published in final edited form as:
J Comp Neurol. 2010 June 15; 518(12): 2382–2404. doi:10.1002/cne.22339.

Bilateral Effects of Unilateral Cochlear Implantation in Congenitally Deaf Cats

Jahn N. O'Neil[1], **Charles J. Limb**[1], **Christa A. Baker**[1], and **David K. Ryugo**[1,2,*]

[1]Department of Otolaryngology-Head and Neck Surgery, Johns Hopkins University School of Medicine, Baltimore, Maryland 21205

[2]Department of Neuroscience, Johns Hopkins University School of Medicine, Baltimore, Maryland 21205

Abstract

Congenital deafness results in synaptic abnormalities in auditory nerve endings. These abnormalities are most prominent in terminals called endbulbs of Held, which are large, axosomatic synaptic endings whose size and evolutionary conservation emphasize their importance. Transmission jitter, delay, or failures, which would corrupt the processing of timing information, are possible consequences of the perturbations at this synaptic junction. We sought to determine whether electrical stimulation of the congenitally deaf auditory system via cochlear implants would restore the endbulb synapses to their normal morphology. Three and 6-month-old congenitally deaf cats received unilateral cochlear implants and were stimulated for a period of 10–19 weeks by using human speech processors. Implanted cats exhibited acoustic startle responses and were trained to approach their food dish in response to a specific acoustic stimulus. Endbulb synapses were examined by using serial section electron microscopy from cohorts of cats with normal hearing, congenital deafness, or congenital deafness with a cochlear implant. Synapse restoration was evident in endbulb synapses on the stimulated side of cats implanted at 3 months of age but not at 6 months. In the young implanted cats, post-synaptic densities exhibited normal size, shape, and distribution, and synaptic vesicles had density values typical of hearing cats. Synapses of the contralateral auditory nerve in early implanted cats also exhibited synapses with more normal structural features. These results demonstrate that electrical stimulation with a cochlear implant can help preserve central auditory synapses through direct and indirect pathways in an age-dependent fashion.

Keywords

auditory; auditory nerve; cochlear nucleus; deafness; synapse; ultrastructure

Auditory deprivation in the developing animal produces striking abnormalities in the auditory pathways, whereas in older animals the effects are much reduced (Powell and Erulkar, 1962; Trune, 1982; Rubel and Fritzsch, 2002; Zhang et al., 2002). These observations are relevant to the age-dependent benefits of cochlear implantation in congenitally deaf humans whereby younger children gain more benefit than older children, and individuals who lose hearing after developing speech are the best candidates for cochlear implants (Waltzman et al., 1994, 1997). The conclusion emerges that an

*CORRESPONDENCE TO: David K. Ryugo, Center for Hearing and Balance, Johns Hopkins University School of Medicine, 720 Rutland Ave., Traylor Research Building, Rm 510, Baltimore, MD 21205. dryugo@jhu.edu.

experience-dependent critical period exists during which some sound stimulation is necessary for the normal development and function of the central auditory system.

Abnormal synaptic structure in auditory nerve endings appears as an early manifestation of congenital deafness in the central nervous system (Ryugo et al., 1997, 1998; Lee et al., 2003). These abnormalities are most prominent in the auditory nerve terminal called the endbulb of Held (Ryugo et al., 1997; Redd et al., 2000, 2002). End-bulbs are large, highly branched axosomatic endings with 500–2,000 release sites (Ryugo et al., 1996); they mediate the faithful transmission of auditory nerve signals to second-order neurons of the cochlear nucleus (CN; Pfeiffer, 1966; Babalian et al., 2003). Ultrastructurally, postsynaptic densities (PSDs) in endbulbs of normal hearing cats are small and dome-shaped, whereas those in deaf animals tend to be larger and flatter. Similar pathologic changes in endbulb morphology have also been observed in the congenitally deaf guinea pig (Gulley et al., 1978) and mouse (Limb and Ryugo, 2000; Lee et al., 2003).

In the context of deafness, synaptic alterations are critical to interventions for compensating hearing loss. Restoration of auditory input must be considered in the context of deprivation-induced changes in morphology and function. If such pathologies at the endbulb synapse are permanent, they could interfere with auditory processing when a cochlear implant is used. If they are not permanent, elucidating the time course and extent to which they are malleable is important. The restoration of physiological attributes has been reported under controlled experimental conditions in which congenitally deaf cats undergo cochlear implantation (Klinke et al., 1999). Consistent with clinical observations in humans who have received cochlear implants (Sharma et al., 2002), the restorative effects of implantation on the auditory cortex of congenitally deaf cats diminish in progressively older animals (Kral et al., 2001). These findings suggest that the critical period of heightened plasticity in early development is dependent upon afferent input and that the end of the critical period marks the time when auditory restoration has diminished effects.

We investigated synaptic plasticity in the endbulb of congenitally deaf white cats following the introduction of auditory nerve activity through cochlear implants at age 3 and 6 months. Bilaterally deaf cats underwent unilateral cochlear implantation followed by a 3-month period of auditory stimulation. We examined ipsilateral auditory nerve synapse structure including the PSD area and curvature, synaptic vesicle concentration, and mitochondrial volume fraction. In addition, we studied the corresponding contra-lateral auditory nerve to investigate the possibility of bilateral effects following unilateral cochlear implantation.

MATERIALS AND METHODS

Subjects

Twenty-four cats were used in this study, as summarized in Table 1. Cochlear implants were surgically inserted into eight congenitally deaf white cats (Kretzmer et al., 2004). An additional seven congenitally deaf white cats and nine normal hearing cats served as unimplanted controls. Three of the normal hearing cats were white litter-mates of deaf cats. All protocols and procedures were in accordance with NIH guidelines and were approved by the Johns Hopkins University Animal Care and Use Committee.

Hearing assessment

Because not all white cats born in our colony are deaf, we assessed each kitten's hearing at 30 and 60 days of age by using standard auditory brainstem responses (ABRs; Ryugo et al., 2003). By this age, mesenchyme has cleared from the middle ear and the external ear is patent to the tympanic membrane (Ryugo et al., 2003). ABRs were obtained in Matlab (MathWorks, Natick, MA) on Tucker-Davis hardware (Alachua, FL). The maximum output

of the free-field speaker is approximately 100 dB SPL (relative to 0.0002 dynes/cm^2) at 16 kHz, as measured by a calibrating microphone placed in the headrest.

Kittens were anesthetized with IM injections of 0.5 mg/kg xylazine and 0.15 mg/kg ketamine hydrochloride. Subcutaneous recording electrodes were inserted caudal and rostral to the pinna on both sides. A grounding electrode was inserted in the neck. Differential potentials were measured across each pinna, referenced to the ground electrode. Tone or click stimuli were presented bilaterally at increasing levels through a free-field speaker (Radio Shack, Fort Worth, TX), and responses were averaged across 1,000 presentations. Deafness was defined as the absence of evoked potentials at sound levels of 95 dB SPL. We previously reported that kittens from our colony of white cats showed no evidence of progressive hearing loss because ABR responses remained constant across 30, 60, 90, 120, 150, and 180 days of age (Ryugo et al., 2003). We therefore inferred that those kittens identified as profoundly deaf at 30 days of age were congenitally deaf.

Cochlear implants

Bilaterally deaf kittens were surgically fitted with a six-electrode unilateral cochlear implant (Advanced Bionics, Sylmar, CA) containing a *Clarion II Hi-Res* type receiver with a custom electrode at 3 (n = 6) or 6 (n = 2) months of age. One cat received a *Clarion 1.2* cochlear implant (CIK-5). The age of 3 months was chosen because endbulbs have not yet reached full maturity (Ryugo and Fekete, 1982), and because at this age the skull of the kitten becomes large enough to support the implant receiver and the kitten itself is strong enough to survive the surgery. Six months was selected because domestic cats reach puberty between 5 and 9 months of age (Fox et al., 2002), a developmental period during which cochlear implantation of humans offers only limited benefits (Snik et al., 1997) and when abnormal synaptic structure is fully evident in auditory nerve fibers of congenitally deaf cats (Ryugo et al., 1997).

Surgical placement of the receiver on the skull and the surgical approach to the round window were performed under general anesthesia and sterile technique. The receiver was fixed onto the skull with sutures anchored through holes drilled in the orbital ridge and by looping suture thread through the zygomatic arch on both sides. Great care was taken to avoid the facial nerve during the approach to the cochlea. The facial nerve exits the temporal bone through the stylomastoid foramen, which in the cat is a small fenestration in the bulla a few millimeters posterior to the external auditory canal. The electrode array was inserted into the round window and advanced as far as possible. The bulla was then filled with soft tissue and the wire was secured to muscle in order to stabilize the electrode position.

The electrode array was 6 mm long. Radiographic analysis confirmed that the electrode array was within the cochlea, with the most basal (sixth) electrode near the round window (Kretzmer et al., 2004). Based on the mean length of a typical cat organ of Corti (24.8 ± 1.1 mm, Liberman, 1982), we calculated that the implant electrodes were situated along the basal 25% of the cochleae. This region is most sensitive to frequencies of 13 kHz and higher (Liberman, 1982). The ages at surgery, implant activation, and termination for each subject are listed in Table 1.

Approximately 2 weeks after surgery, the impedance of individual electrodes was determined by using electrical field imaging (EFI) software (Advanced Bionics). Normal functioning electrodes had impedances of <10 kΩ. Upon initial activation, electrode stimulation elicited pupil dilation, head searching movements, and/or pinna flicks in the animal. Optimization of stimulation intensity was achieved by increasing the stimulation level up to the point where the subject crouched, vocalized, or extended its claws. This point was defined as the maximum stimulation level, and the intensity was reduced until these

responses subsided (defined as the C or comfort level; Shapiro, 2006). The presence of electrically evoked compound action potentials (eCAPs) further indicated that implant stimulation was sending activity into the brain (Fig. 1).

At the time of surgery, all implant leads were inserted as far as possible into the round window. Each implant was tested twice monthly so that adjustments could be made if and when electrode thresholds changed. Testing also informed us when electrodes became nonfunctional. We determined that at least three functional electrodes were active during each cat's stimulation program except for one cat whose device was never activated (Table 1).

It is axiomatic that cat behavior varied considerably from animal to animal. Our implanted cats did not seem to differ from age-matched controls in their play behavior or tendency to sleep for extended periods during the day. There are, however, some observations that merit additional comment. Our deaf cats, especially when young, emit abnormally loud vocalizations with a voice quality that resembles the howl of female cats in estrus. Because such calls are made by both male and female kittens, estrus is, however, not the cause. The frequency of such vocalizations diminishes as deaf cats mature and/or after their cochlear implant is activated.

It seems that all cats, hearing or deaf, exhibit spontaneous movements of their pinnae. Only hearing and coch-lear implanted cats display sound-evoked pinna movement. Cats with cochlear implants are clearly able to hear environmental sounds, although we do not know the extent to which they are capable of distinguishing the fine timing cues required for sound localization.

Environmental sounds are detected by a microphone and delivered to a sound processor by which the signals are translated into biphasic electrical impulses at each electrode. The stimulation paradigm is a modification of the continuous interleaved strategy (CIS; Wilson et al., 1991), using >3,000-Hz carrier rate, biphasic pulses amplitude-modulated by bandpass filtering, and distributed across the active electrodes (Advanced Bionics, HiRes software). Electrodes are activated in a monopolar configuration. Cats carried the processor in a backpack 5 days a week, approximately 7 hours a day, during which time they interacted with lab personnel, and were fed, handled, and exposed to a variety of sounds including human speech and radio programming. In addition to passive listening, cats learned to approach their food bowl when a specific acoustic stimulus was played (Supplemental movie S1, Ryugo et al., 2005). Once or twice per day, the specific stimulus was played intermixed with other stimuli, and if the cat approached the food bowl immediately after the appropriate stimulus, it received a small food reward.

Tissue preparation

At the end of the stimulation period, the cats were euthanized by administration of a lethal dose of sodium pentobarbital (55–75 mg/kg, IP). When fully anesthetized, cats were administered the anticoagulant heparin and perfused through the heart with 25 ml of 0.1 M phosphate-buffered saline containing 0.1% sodium nitrite, followed by 1.5 liters of a standard fixative (2% glutaraldehyde, 2% paraformaldehyde fixative in 0.1 M phosphate buffer, pH 7.4).

After removal of the implant receiver, the cranium was opened so that the brain and cochleae were exposed. The stapes was removed, and fixative was gently injected into the round window and out the oval window of each cochlea. The head (with brain and cochleae) was immersed in fresh fixative overnight. The following day, the brain was removed from the skull, and the CN was isolated, blocked, and cut coronally (transversely) on a

Vibratome. Every third section through the CN was cut at 75 μm, osmicated (1% osmium tetroxide, 15 minutes), and stained en bloc with 1% uranyl acetate (overnight). Sections were then rinsed in maleate buffer, dehydrated, infiltrated with Epon, and embedded in Epon between two sheets of Aclar. Remaining sections were cut at 50 μm and stained with cresyl violet for observation under the light microscope.

Cochleae were processed independently of the brainstem. Briefly, each cochlea was perfused with the same fixative, osmicated, rinsed, dehydrated, and embedded in Araldite. Sections were collected (20–40 μm thickness) and stained with toluidine blue. A separate manuscript that relates ganglion cell survival to stimulation parameters and brain plasticity is being prepared.

Microscopy

Based on the position of the implant electrode in the cochlea, we selected the corresponding frequency region (13 kHz and higher) in the anteroventral cochlear nucleus (AVCN; Bourk et al., 1981; Ryugo and May, 1993) for analysis by light and electron microscopy. In coronal sections, this region represented the dorsal third of the AVCN and included the posterior and posterodorsal parts of the anterior division (Brawer et al., 1974). We wanted to ensure that we studied cells and endings in the region that was directly stimulated by the cochlear implant because differential effects of stimulation have been demonstrated in stimulated and unstimulated parts of the CN (Kawano et al., 1996, 1997). Tissue sections were first examined by using a light microscope. In the AVCN, large (20–30 μm in diameter) cells with a pale, centrally located nucleus, a perinuclear cap of Nissl substance, and a “necklace” of Nissl bodies were evident, characteristic of spherical bushy cells (SBCs; Osen, 1969). Such cells in the region above the 13-kHz isofrequency contour (Bourk et al., 1981) were drawn by using oil immersion objectives (100×, NA = 1.3) and a drawing tube (see Table 5 for numbers of cells sampled).

The sections containing structures to be studied by using an electron microscope were drawn and mapped with respect to tissue landmarks by using a light microscope and drawing tube. Select regions were divided into two or three pieces by using razor cuts, and embedded in a BEEM capsule. The location of interest was trimmed and photographed. Serial sections (~75 nm) were cut on an ultramicrotome, collected on Formvar-coated slot grids, and further stained with uranyl acetate and lead citrate for electron microscopy.

SBCs were identified by the relatively smooth cell outline, the presence of a centrally located, pale, round nucleus, and distinct Nissl bodies (stacks of endoplasmic reticulum seen under an electron microscope) in the cytoplasm and around one pole of the nucleus (Lenn and Reese, 1966; Osen, 1969; Cant and Morest, 1979). Cells were chosen in which the nucleolus was plainly visible. Endbulbs were identified by their location on the cell body, large round synaptic vesicles, clear cytoplasm, and distinct synaptic curvature. The cells and endings that met these criteria and were free of debris were selected for study.

Endbulbs were photographed at 14,000× (JEOL 100CX microscope, Pleasanton, CA) or 15,000× (H-7600 Hitachi microscope, Tokyo, Japan). Micrographs were scanned and digitized from negatives (JEOL) or collected with a digital camera (2k × 2k AMT XR-41M bottom mount). The scale for each method of digitization was obtained by using a calibrated submicron grid (Electron Microscopy Supply, Fort Washington, PA). This grid was photographed on the microscope after each change of the microscope filament to ensure consistency across time. Two or three endings on 5–10 different SBCs were followed through 10–30 serial sections.

Reconstruction of endbulbs and PSDs

Only part of the endbulb is seen in electron micrographs because endbulbs of Held are highly branched structures, the tissue sections are very thin, and the magnification is relatively high. These parts are referred to as "profiles" (Ryugo et al., 2006). Endbulb profiles and PSDs were identified in consecutive electron micrographs in which PSDs appear as dome-shaped asymmetric thickenings of the postsynaptic membrane that are associated with clear, round synaptic vesicles on the presynaptic side. Only PSDs that occurred in two or more consecutive sections were included for analysis.

Endbulb profiles and PSDs were reconstructed in three dimensions and measured by using commercially available software (Amira, Berlin, Germany). Briefly, endbulb profiles and PSDs were traced in consecutive sections by using Adobe Photoshop CS3 (San Jose, CA) and then aligned and stacked by using mitochondria and the endbulb profile as fiducial marks. The stack was then exported to Amira to yield a voxel-based representation and rotated so that the SBC surface lying beneath the endbulb was viewed en face. Each PSD was segmented into an individual three-dimensional "patch" and its surface area calculated. The presentation of these patches (as in the figures) is restricted to an en face view that provides a flattened two-dimensional appearance.

PSD curvature

The three-dimensional shape of the PSD has been characterized as having "small projections" (Lenn and Reese, 1966), as being "convex" toward the presynaptic terminal (Rees et al., 1985), and as being "arched toward the end-bulb" (Cant and Morest, 1979). We quantified the degree of curvature (Fig. 2) of endbulb synapses for each of the cohorts of treatment conditions by using the method of Cooke et al. (1974). The chord length and perpendicular height of individual PSDs were measured in the midpoint of each synapse by using ImageJ (NIH, Bethesda, MD).

Endbulb morphometric analysis

Based on the maturational changes observed in endbulb structure (Jhaveri and Morest, 1982a,b; Neises et al., 1982; Limb and Ryugo, 2000; Ryugo et al., 2006), we also examined mitochondrial volume fraction and synaptic vesicle density. A minimum of 10 endbulb profiles from each animal was used for morphometric analysis. For each endbulb profile, measurements were collected to determine *mitochondrial volume fraction* (mitochondria area divided by profile area, multiplied by 100%; Black et al., 1991) and *synaptic vesicle density* (the number of synaptic vesicles per μm^2 as measured within 0.5 μm of the PSD; see Fig. 1 of Ryugo et al., 2006).

The counts were "corrected" according to a modification of Abercrombie's (1946) formulation. Because synaptic vesicles (SVs) appear ring-shaped in cross section, we only counted structures that exhibited a complete ring, had a clear lumen, and were <80 nm in diameter. Those SVs whose luminal points were outside the ultrathin section, but that were nevertheless represented by fragments inside the section, had their luminal points extending through a volume of tissue equivalent to, on average, the inside diameter of the SV. SV fragments without a lumen were effectively ignored, so the outside diameter of the SV was not used in the correction formula. We measured the inside diameter of SVs (range 79–337) associated with 10–82 PSDs from a minimum of five endbulbs per animal. The mean inside diameter, M, was used in the formula $P = A(T/T + M)$ to calculate the corrected count P where A equals the uncorrected count and T equals the ultrathin section thickness.

The measured values were grouped with respect to the following cohorts: hearing, deaf, and cochlear-implanted. Data from cochlear-implanted cats were further divided into a

stimulated group: 3-month ipsilateral, 3-month contralateral, 6-month ipsilateral, 6-month contralateral; and a nonstimulated group: 3-month implanted control. Photomicrographs were adjusted only for contrast and brightness by using Adobe Photoshop CS3.

Statistics

The nonparametric Kruskal-Wallis statistical test was used for analyzing PSD size, curvature, and SV density because the measured values did not exhibit a normal distribution. In other instances (see text), we applied multivariable ANOVA and Tukey-Hanson HDS tests. These tests incorporated the Bonferroni adjustment for multiple comparison procedures. Means and standard deviations are provided in the text and tables; means and standard errors of the mean are shown in the figures.

RESULTS

Status of cochleae

Verification of cochlear implant electrode placement was confirmed in every case by radiographic examination and histologic demonstration of “scar” tissue within the scala tympani. As previously reported for deaf white cats, there was a complete absence of receptor hair cells (Mair, 1973; Ryugo et al., 1997, 1998). The organ of Corti appeared as an undifferentiated mass of cells, encased by the remnants of the collapsed Reissner's membrane. Essentially, the scala media was obliterated. Counts of spiral ganglion cells were made for each cochlea when possible. For all of our deaf cats (implanted or not), spiral ganglion cell number ranged from 11,090 to 48,192. There was no relationship between the number of surviving ganglion cells and synapse restoration (Chen and Ryugo, unpublished observations), and a full description of cochlear implantation, cochlear histology, and spiral ganglion cell survival will be presented in a separate report.

Endbulb morphology in normal hearing and deaf cats

Endbulbs and their synapses in 6-month and older normal hearing and deaf cats were examined to establish morphologic baselines with which to compare the effects of cochlear implantation. In normal hearing cats, endbulb profiles were found on SBCs (Fig. 3A–D). Auditory nerve endings were identified by the accumulation of clear, round SVs and the associated pre- and postsynaptic membrane thickenings. We focused on the postsynaptic membrane thickening or density because it was prominent and therefore easy to find. The PSD was characteristically dome-shaped (for mean curvature, see Table 4) and bulged into the presynaptic endbulb. The SVs were large (approximately 50 nm in diameter) and had a density of 45.0 ± 12.4 vesicles per μm^2. Multiple PSDs were found on each endbulb, typically spanning 2–10 consecutive sections (mean = 4.9 ± 2.1). These PSDs were discrete and relatively uniform in size and distribution (Fig. 3A′–D′). The average size of individually reconstructed PSDs was 0.122 ± 0.07 μm^2 (n = 175; see Fig. 10 and Table 2).

Average mitochondrial volume fraction was calculated to be 19.5 ± 7.1%. The membrane apposition between the endbulb and SBC generally but not always exhibited an intercellular space or cistern. This space often contained a glial process. The cisternae could be followed through serial sections to form a network of channels. Endbulb morphology of the 6-month-old cats resembled that of older adult cats (Lenn and Reese, 1966; Cant and Morest, 1979; Ryugo et al., 2006), and endbulbs were consistently associated with cell bodies characterized as SBCs (Cant and Morest, 1979; Ryugo and Sento, 1991).

In the congenitally deaf adult cat, endbulbs retain many of the features found in the normal hearing cat. They form prominent contacts on the somata of SBCs and contain large round SVs (Ryugo et al., 1997, 1998). Distinctly abnormal features of endbulbs in deaf cats

include the appearance of longer, flattened PSDs (mean curvature is statistically different from normal; see Table 4), a lack of intercellular cisternae, and increased clustering of SVs in the immediate vicinity of the PSDs (Fig. 4). Some abnormal PSDs in the deaf cat spanned the entire series of consecutive sections, although PSDs having normal features and sizes were also observed. The striking size increase for many PSDs was reflected by a statistically larger mean (0.269 ± 0.36 μm^2, n = 223, $P < 0.01$, Kruskal-Wallis tests; see Fig. 10, Table 2). An elongation of the PSDs tended to occur along the long axis of the endbulb processes. There was also a notable increase in SV density (63.0 ± 41.8 vesicles per μm^2) compared with that of endbulbs from normal hearing cats (45.0 ± 12.4, $P < 0.01$, Kruskal-Wallis tests). Mitochondrial volume fraction was 19.2 ± 9.8%, a measure that did not statistically differ across cohorts.

Cochlear implant cats

Eight congenitally deaf cats were implanted in the left cochlea. Six cats were implanted at approximately 3 months of age (75–97 days), and two were implanted at approximately 6 months (163 and 173 days). The device failed prior to activation in one cat (CIK-7) implanted at 89 days, and this cat became our nonactivated implant control to evaluate possible nonspecific effects of surgery. Electrically evoked compound action potentials (eCAPs) were recorded from the operational electrodes (Fig. 1), and stimulus-response curves indicated evoked activity in the auditory nerve (Kretzmer et al., 2004). All implanted cats exhibited startle responses to sudden and loud sounds when the device was turned on; no sound-related responses could be elicited when the device was not active. Importantly, cats with functional implants learned to approach their food bowl when presented with a unique computer-generated sound that signaled a food reward. These cats ignored sounds (banging, bird calls, and whistling) that were not paired with food. Cats were under constant supervision during stimulation. We did not discern any remarkable differences in behavior between the early and late implanted cats.

Auditory nerve endings ipsilateral to the cochlear implant (implanted at 3 months)—Endbulb profiles were readily apparent on the somata of SBCs. The most prominent result of cochlear implantation after 3 months of stimulation was the obvious return of the small, dome-shaped PSDs (Fig. 5A,B; mean PSD curvature, see Table 4). Stimulation also returned SV density back to normal levels on the ipsilateral side (42.0 ± 30.8 vesicles per μm^2) compared with hearing cats. Mitochondrial volume fraction was 18.7 ± 9.5%. Large round SVs were clustered around the PSDs, and more than half of the profiles exhibited cisternae. The reconstructed PSDs (Fig. 5A′,B′) of implanted cats returned to the size (0.100 ± 0.08 μm^2, n = 252; see Table 2 and Fig. 10) typical of normal hearing cats. These PSDs were significantly smaller ($P < 0.01$, Kruskal-Wallis tests) than those of congenitally deaf cats, late implanted deaf cats, and the nonactivated implanted control cat.

Auditory nerve endings contralateral to the cochlear implant (implanted at 3 months)—Endbulb morphology contralateral to the cochlear implant exhibited features found in deaf and in normal hearing cats. Punctate, curved synapses typical for endbulbs of hearing cats were plentiful. In addition, there were also numerous long flattened synapses as seen in deaf cats (Fig. 6 A,B). There was, however, no statistical difference in SV density (45.2 ± 13.5 vesicles per μm^2) within 0.5 μm of the PSD or the mitochondrial volume fraction (20.8 ± 8.6%) compared with normal hearing cats or ipsilaterally stimulated cats (see Fig. 10). Reconstruction of PSDs through serial sections revealed that, on average, many of the PSDs were larger than those seen in normal hearing cats but smaller than those seen in congenitally deaf cats (Fig. 6A′,B′). The mean curvature of PSDs was significantly less than that of hearing or early ipsilateral CI cats ($P < 0.01$, Kruskal-Wallis tests; see Table

4). The mean size of the PSDs (0.187 ± 0.17 μm^2, n = 199) was between the group of normal hearing cats and the group of congenitally deaf cats (see Fig. 10).

Auditory nerve endings ipsilateral to the cochlear implant (implanted at 6 months)—Endbulb synapses were reconstructed and analyzed in two cats that were implanted at 6 months of age. The question was whether this later activation of the auditory nerve by cochlear implants would also have a "restorative" effect on synapses of congenitally deaf cats. As in normal hearing cats, many synapses exhibited dome-shaped PSDs (Fig. 7A,B). The main difference was that the PSDs appeared longer. When reconstructed through serial sections (Fig. 7A′,B′), the average PSD area was larger (0.274 ± 0.29 μm^2, n = 123; see Fig. 10) and less curved than that of normal hearing cats ($P < 0.01$, Kruskal-Wallis tests; see Table 4). Mitochondrial volume fraction averaged 22.8 ± 7.4% and SV density 67.9 ± 15.1 vesicles per μm^2. The synapses in the late implanted cats resembled, on average, those of congenitally deaf cats with no implants. That is, the structural features that were quantified (e.g., PSD size and curvature, synaptic vesicle density, mitochondrial volume fraction, SBC size) had similar values. Qualitatively, however, synapses were still recognizable as synapses.

Auditory nerve endings contralateral to the cochlear implant (implanted at 6 months)—Endbulb synapses were analyzed in the CN contralateral to the cochlear implant in the cats activated at 6 months of age. The synapses in these endbulbs had the same morphology as those of congenitally deaf cats that did not receive a cochlear implant (Fig. 8). They exhibited asymmetric PSDs that were relatively flat (Table 4) and large (0.249 ± 0.47 μm^2, n = 110; see Fig. 10) and statistically different from those of normal hearing and early implanted (ipsilateral) cats ($P < 0.01$, Kruskal-Wallis tests). Mean mitochondrial volume fraction was 23.6 ± 15.2% and SV density was 61.1 ± 18.5 vesicles per μm^2 (see Fig. 10).

Endings from a single unstimulated cat—One cat received a cochlear implant in which the impedance of every electrode was abnormally high, and eCAPs could not be elicited. Moreover, this cat did not have the pinna movements normally associated with implant activation. Although radiographs indicated that the electrode array was located within the cochlea, no further attempt was made to stimulate this cat after the initial activation failure, so this animal was used as an implanted control. After a 3-month postimplant survival period, auditory nerve synapses were examined to determine the effects of surgery, special handling, and minimal stimulation. Endings ipsilateral to the unstimulated implant were similar to those seen in deaf cats (Fig. 9). The mean PSD areas ipsilateral (0.306 ± 0.44 μm^2, n = 38) and contralateral (0.265 ± 0.32 μm^2, n = 37) to the cochlear implant were not different from each other but were statistically larger than those of normal hearing cats ($P < 0.01$, Kruskal-Wallis tests). Mean values for mitochondrial volume fraction and SV density were similar to those of deaf cats (Fig. 10).

Summary of PSD data

Analysis of PSDs associated with auditory nerve fibers in the CN was conducted in seven cohorts of cats (Fig. 10, Table 2). PSD size and curvature were statistically similar in normal hearing and the ipsilateral CN of 3-month-old cochlear implanted congenitally deaf cats. The PSDs in these two cohorts were statistically different from those of congenitally deaf cats, an implanted but never activated control cat, and congenitally deaf cats implanted at 6 months of age ($P < 0.01$, Kruskal-Wallis tests). The size of PSDs in the CN contralateral to the early-activated cochlear implant was statistically in between these two groupings.

The duration of deafness is a variable that is known to affect ganglion cell survival (Mair, 1973; Keithley and Feldman, 1979; Nadol and Eddington, 2006; Leake et al., 2007). This variable is not, however, correlated with PSD size when the effects of electrical stimulation via a coch-lear implant are considered (Fig. 11). We determined that the size of PSDs is related to early implantation ($P < 0.0001$) and not to the total stimulation hours ($P = 0.582$) or the number of active electrodes ($P = 0.426$; Fig. 12, Table 3). Because the sample size of each cohort was different, we plotted all PSD values from each of the cats (Fig. 13). In this way, we show that the results are not caused by data "weighting" from a few subjects. Moreover, analysis within cohorts showed that there were no differences in PSD size among individual cats within a cohort ($P = 0.42$, ANOVA). Collectively, the data suggest that early electrical stimulation through cochlear implantation is the key variable that influences the size and shape of auditory nerve synapses.

PSD curvature

The curvature formula of Cooke et al. (1974) was used to indicate curvature. An increasing positive value indicated positive curvature. Normal hearing cats have endbulb synapses exhibiting more positive curvature and thus greater convexity into the endbulb than congenitally deaf cats ($P < 0.01$, ANOVA). The PSDs ipsilateral to the cochlear implant in early implanted cats exhibit curvature values similar to those of normal cats but statistically different from those of the other cohorts (Table 4).

Cisternae

Extracellular cisternae are commonly observed between the presynaptic terminal of auditory nerve fibers and the postsynaptic SBC (Lenn and Reese, 1966; Redd et al., 2000; Lee et al., 2003). Astrocytic processes can also be found within the cisternae. These cisternae could represent a fixation artifact, but such a conclusion seems unlikely because so many other structures within the immediate vicinity exhibit fine preservation (Lenn and Reese, 1966). In our material, the auditory nerve endings of normal hearing cats exhibit, on average, 2.03 (±0.84) cisternae (Fig. 3, arrows). In contrast, those auditory nerve endings of congenitally deaf cats have significantly fewer cisternae (0.48 ± 63), even with a cochlear implant (0.56 ± 1.39, $P < 0.05$, ANOVA). These data suggest that there is no restoration of cisternae with cochlear implant use, even when stimulation begins at 3 months.

Endbulb morphometric analysis

We analyzed mitochondrial volume fraction and SV density for the auditory nerve in the seven cohorts. Mitochondria content is hypothesized to reflect metabolic needs and synaptic activity. We proposed that the separate cohorts would exhibit different values for mitochondrial volume fractions. In fact, we observed no differences in mitochondrial volume fraction among the cohorts ($P = 0.48$, Tukey-Hanson HDS tests; Fig. 10). Deaf animals were found to have significantly more SVs than normal animals, and early cochlear implantation returned these values to normal levels for both the ipsilateral and contra-lateral auditory nerve endings ($P < 0.002$, Kruskal-Wallis tests). Late implanted animals and the inactivated control animal exhibited SV densities whose values were statistically the same as those of congenitally deaf animals.

Effects on spherical bushy cells

The adverse effects of auditory deprivation on the development of the auditory pathways are well documented (e.g., Rubel et al., 1984). Chronic electrical stimulation of the ear has been employed in an attempt to prevent atrophy of the developing auditory system (Chouard et al., 1983). More recently, the use of electrical stimulation on the deaf auditory pathway has yielded conflicting observations: there are reports that somatic size in the CN is unaffected

by electrical stimulation (Hultcrantz et al., 1991; Ni et al., 1993; Coco et al., 2007), whereas others report modest but significant increases in somatic size and density (Lustig et al., 1994; Leake et al., 1999). Because these studies were conducted in cats that were ototoxically deafened as kittens, we sought to readdress this issue by using our cats that have inherited congenital deafness.

SBCs from the high-frequency region (13 kHz and higher) of the AVCN were analyzed from seven cohorts: normal hearing, congenitally deaf, nonactivated implanted control, and ipsilateral and contralateral early and late implanted cats (Fig. 10, Table 5). Congenitally deaf cats, regardless of treatment, exhibit a >31% loss in somatic size. SBCs of deaf cats were significantly smaller than those of normal hearing cats ($P < 0.05$, Tukey-Hanson HSD tests), and stimulation via cochlear implantation did not result in larger SBC size.

Functional assessment

We compared representative evoked auditory brainstem responses (EABRs) from normal, acutely deafened cats, congenitally deaf cats that were stimulated via cochlear implants, and congenitally deaf white cats (Fig. 14). It must be noted here that the collection of EABRs using cochlear implants is extremely difficult due to the large stimulus artifact created by the RF signal from the cochlear implant transmitter. Nevertheless, by aligning the first peaks of the response (attributable to the auditory nerve response), two key points can be made regarding the EABRs recorded in congenitally deaf animals. First, in the untreated deaf cats (bottom traces), all responses downstream from the auditory nerve are small and delayed in latency. Second, whereas cochlear implantation does not restore the EABR to its normal appearance, its waveform in the implanted cats exhibits more distinct response peaks in comparison with long-term deafened cats. These results suggest that some degree of synchronous transmission is preserved by stimulation through the cochlear implant.

DISCUSSION

The present results demonstrate that early electrical stimulation with a unilateral cochlear implant has a dramatic effect on auditory nerve synapses in congenitally deaf cats. Activation of auditory nerve fibers by a cochlear implant at 3 months of age restored some key features of synaptic morphology, whereas activation at 6 months of age had no effect. These data are consistent with the concept of a “critical” or sensitive period for plasticity and its time course in auditory (2–5.5-month-old cats; Kral et al., 2002) and visual (4–8-month-old cats, Cynader and Mitchell, 1980) cortex. In addition, moderate corrective effects on auditory nerve synapses were observed in the contralateral CN that was not directly stimulated by the implant. Our results show an age-dependent interval for plasticity in the central auditory system that is mediated by both direct and indirect pathways.

Activity and PSDs in spherical bushy cells

In auditory nerve fibers of congenitally deaf cats, the lack of spontaneous and sound-evoked activity caused a significant increase in PSD size (Ryugo et al., 1998). In cats with elevated thresholds (60–75 dB hearing loss), spontaneous activity plus activity evoked by loud sounds resulted in a more modest hypertrophy of PSDs. Rats housed in a quiet room experienced normal spontaneous activity but minimal evoked activity and showed an increased PSD size (Rees et al., 1985). These findings indicate that PSD size in endbulbs is inversely proportional to the amount of spike activity in the parent fiber.

Synaptic strength and plasticity have been studied in other central synapses such as CA1 in the rat hippocampus, in which it was shown that the size of PSDs increases in response to pharmacological blockade of spike activity (e.g., Murthy et al., 2001; Qin et al., 2001; Yasui

et al., 2005). Quiescent synapses exhibited larger PSDs and increased numbers of SVs, and were accompanied by increases in synaptic strength. Consistent with this correlation, an increase in synaptic strength is seen in the AVCN of the congenitally deaf mouse compared with that of normal hearing mice (Oleskevich and Walmsley, 2002; Oleskevich et al., 2004). This increase in synaptic strength may be related to an increase in transmitter receptors that become distributed in the hypertrophied PSDs (e.g., Whiting et al., 2009). These adjustments in response to perturbations in activity appear to reflect compensatory mechanisms that have been referred to as homeostatic scaling (Turrigiano and Nelson, 2004). Brain homeostasis seeks to allow neurons to maintain circuit stability by adjusting their set-point to accommodate changes in excitatory and/or inhibitory activity.

Mitochondria and synaptic vesicle morphometrics

Mitochondrial content within synaptic endings was correlated to the metabolic needs of the developing neuron (Ryugo et al., 2006) as reflected by a growth of spike activity in individual auditory nerve fibers (Brugge et al., 1981; Romand and Romand, 1982; Walsh and McGee, 1987). In this context, we proposed that the mitochondrial volume fraction would be higher in auditory nerve endings of normal hearing animals and congenitally deaf animals that received stimulation from a cochlear implant compared with that in congenitally deaf animals. We observed, however, no difference in mitochondrial volume fraction among normal hearing, congenitally deaf, and cochlear-implanted cats. Variations in metabolic demands can apparently be met without altering the mitochondrial volume fraction, perhaps by adjusting the surface area of the cristae or enzymatic activity.

SVs represent the substrates of chemical transmission and were predicted to change in number following deafness. We included only those counts of SVs that fell within 0.5 μm of the PSD using the rationale that proximity to the PSD suggested a releasable pool of SVs (Zenisek et al., 2000). SV density was lower in normal hearing animals and congenitally deaf animals implanted at 3 months of age but greater in congenitally deaf cats, late implanted cats, and the implanted control. The lack of activity apparently caused an increase in SV concentration. More vesicles would presumably improve the probability of synaptic transmission if and when a spike discharge invaded the endbulb. We previously reported a loss of SVs in endings of auditory nerve fibers in deaf cats (Ryugo et al., 1997; Redd et al., 2000). The earlier published results reflect differences in methods, criteria, and perhaps inadequate sampling caused by the variability.

Trans-synaptic effects on spherical bushy cells

Spike activity and neural transmission in spiral ganglion cells and their fibers appear essential for the normal development of CN neurons (Rubel and Fritzsch, 2002; West and Harrison, 1973). Given that neuronal atrophy is a major consequence of sensory deprivation, it seems reasonable to predict that increasing neuronal activity should reverse the atrophy. Studies that used ototoxic deafening of normal hearing cats have reported small but positive effects of electrical stimulation on CN cell size (Lustig et al., 1994; Leake et al., 1999; Stakhovskaya et al., 2008), whereas others using similar methods show no effects (Hultcrantz et al., 1991; Ni et al., 1993; Coco et al., 2007). Our data show that electrical stimulation of auditory nerve fibers via cochlear implants had no effect on the size of the SBC neurons in this model of hereditary deafness. Hereditary deafness obviously represents a different model from ototoxic deafness, so it remains to be determined to what extent the results from the separate animal models are comparable.

Critical period

The concept of the critical period has been applied to explain biological phenomena that occur or are most severely affected during a brief period of time during development, such

as “imprinting” (Lorenz, 1935), cortical barrel plasticity (Van der Loos and Woolsey, 1973; Weller and Johnson, 1975), birdsong acquisition (Konishi, 1985), and functional maturation of auditory cortex (Chang and Merzenich, 2003; Zhou et al., 2008). Reports that young children receiving cochlear implants gained far superior benefit compared with older children and adults hinted strongly at a critical period (Quittner and Steck, 1991; Waltzman et al., 1993; Gantz et al., 1994; Tyler and Summerfield, 1996). In congenitally deaf cats, electrical stimulation was reported to recruit auditory cortical responses contingent upon its commencement before 6 months of age (Klinke et al., 2001; Kral et al., 2002). Our data may provide the structural foundation for these observations: 3-month-old cochlear implant recipients exhibited somewhat restored auditory nerve synapses, whereas 6-month-old cochlear implant recipients did not. The developmental period preceding puberty appears most favorable for implant-induced synaptic plasticity, and the restoration of auditory nerve synapses undoubtedly facilitated the delivery of afferent signals to the fore-brain in a timely, coherent, and synchronized way.

Contralateral effects

Endbulbs in the contralateral CN that did not receive direct stimulation by the cochlear implant were expected to provide within-animal control data. However, contralateral auditory nerve synapses in animals implanted at 3 months resembled those of cats born with 60–70-dB hearing loss, not deaf cats (Ryugo et al., 1998). The average size of these PSDs was larger than those of normal hearing cats but not as severely hypertrophied as those of congenitally deaf cats. They were statistically “between” the two groups. We infer that activity in the auditory pathway, initiated by the cochlear implant, partially salvaged auditory nerve synapses on the unimplanted side via input from commissural, olivocochlear, and/or descending pathways (Liberman and Brown, 1986; Wenthold, 1987; Doucet and Ryugo, 2006; Winer, 2006). This “saving” may be relevant to discussions regarding the timing of sequential surgeries to achieve bilateral implants in children (Firszt et al., 2008).

Implications for cochlear implantation

Several abnormalities have been demonstrated in the auditory system following deafness including reduced numbers of spiral ganglion neurons (Mair, 1973; Leake and Hradek, 1988; Heid et al., 1998; Ryugo et al., 1998), abnormal synaptic structure (Ryugo et al., 1997; Redd et al., 2000, 2002; Lee et al., 2003), physiological alterations of auditory nerve responses in the CN (Oleskevich and Walmsley, 2002; Wang and Manis, 2005), and ectopic projections in the ascending pathways (Nordeen et al., 1983; Moore and Kitzes, 1985; Franklin et al., 2006). These changes undoubtedly affected synaptic transmission where degraded responses in the inferior colliculus (Snyder et al., 1999; Vale and Sanes, 2002; Vollmer et al., 2005) and auditory cortex (Kral et al., 2006) have been observed. How these pathologies affect the perception of sound is unknown, but the positive behavioral response of our early and late implanted cats to their “dinner bell” may simply reflect the simplicity of the task.

Endbulbs are implicated in mediating the precise temporal processing of sound (Molnar and Pfeiffer, 1968) and are known to transmit from auditory nerve to postsynaptic cell with a high degree of fidelity (Babalian et al., 2003). Detection and identification of some sounds are not nearly as demanding as the processing of temporal cues needed for sound localization, pattern recognition, or speech comprehension. The introduction of synaptic jitter, delay, or failure by congenital deafness at the end-bulb synapse could compromise such processing. The contribution of electrical activity to synaptic ultrastructure demonstrates that a cochlear implant can reverse some morphologic abnormalities in the auditory pathway when stimulation is started early. Moreover, effects are observed

bilaterally at the earliest stage in the auditory pathway, demonstrating that stimulation has a widespread trophic effect.

Acknowledgments

The authors thank Andre Haenggeli and John Niparko for help with the surgeries; Erika Kretzmer for involvement in the early part of this project; Tan Pongstaporn for contributions with electron microscopy; San-san Yu for technical assistance; and The Listening Center at the Johns Hopkins Hospital for advice on cochlear implant programming in non-lingual subjects. Dr. Limb is a consultant for Advanced Bionics and receives support for unrelated work. Some of these cats contributed data that have been previously published in abbreviated form (Kretzmer et al., 2004; Ryugo et al., 2005).

Grant sponsor: National Institutes of Health; Grant numbers: DC000232, DC00023, DC005211, and EY01765; Grant sponsor: The Emma Liepmann Endowment Fund; Grant sponsor: the Advanced Bionics Corporation.

LITERATURE CITED

Abercrombie M. Estimation of nuclear population from microtome sections. J Anat. 1946; 94:239–247.

Babalian AL, Ryugo DK, Rouiller EM. Discharge properties of identified cochlear nucleus neurons and auditory nerve fibers in response to repetitive electrical stimulation of the auditory nerve. Exp Brain Res. 2003; 153:452–460. [PubMed: 12955378]

Black JE, Zelazny AM, Greenough WT. Capillary and mitochondrial support of neuronal plasticity in adult rat visual cortex. Exp Neurol. 1991; 111:204–209. [PubMed: 1989898]

Bourk TR, Mielcarz JP, Norris BE. Tonotopic organization of the anteroventral cochlear nucleus of the cat. Hear Res. 1981; 4:215–241. [PubMed: 7263511]

Brawer JR, Morest DK, Kane EC. The neuronal architecture of the cochlear nucleus of the cat. J Comp Neurol. 1974; 155:251–300. [PubMed: 4134212]

Brugge JF, Kitzes LM, Javel E. Postnatal development of frequency and intensity sensitivity of neurons in the anteroventral cochlear nucleus of kittens. Hear Res. 1981; 5:217–229. [PubMed: 7309639]

Cant NB, Morest DK. The bushy cells in the anteroventral cochlear nucleus of the cat. A study with the electron microscope. Neuroscience. 1979; 4:1925–1945. [PubMed: 530439]

Chang EF, Merzenich MM. Environmental noise retards auditory cortical development. Science. 2003; 300:498–502. [PubMed: 12702879]

Chouard CH, Meyer B, Josset P, Buche JF. The effect of the acoustic nerve chronic electric stimulation upon the guinea pig cochlear nucleus development. Acta Otolaryngol. 1983; 95:639–645. [PubMed: 6688322]

Coco A, Epp SB, Fallon JB, Xu J, Millard RE, Shepherd RK. Does cochlear implantation and electrical stimulation affect residual hair cells and spiral ganglion neurons? Hear Res. 2007; 225:60–70. [PubMed: 17258411]

Cooke TC, Nolan MT, Dyson ES, Jonas DG. Pentobarbital-induced configurational changes at the synapse. Brain Res. 1974; 76:330–335. [PubMed: 4135928]

Cynader M, Mitchell DE. Prolonged sensitivity to monocular deprivation in dark-reared cats. J Neurophysiol. 1980; 43:1026–1040. [PubMed: 7359175]

Doucet JR, Ryugo DK. Structural and functional classes of multipolar cells in the ventral cochlear nucleus. Anat Rec A Discov Mol Cell Evol Biol. 2006; 288:331–344. [PubMed: 16550550]

Firszt JB, Reeder RM, Skinner MW. Restoring hearing symmetry with two cochlear implants or one cochlear implant and a contralateral hearing aid. J Rehabil Res Dev. 2008; 45:749–767. [PubMed: 18816424]

Fox, JG.; Anderson, LC.; Loew, FM.; Quimby, FW. Laboratory animal medicine. 2nd ed.. Academic Press; London: 2002. p. 466-470.

Franklin SR, Brunso-Bechtold JK, Henkel CK. Unilateral cochlear ablation before hearing onset disrupts the maintenance of dorsal nucleus of the lateral lemniscus projection patterns in the rat inferior colliculus. Neuroscience. 2006; 143:105–115. [PubMed: 16971048]

Gantz BJ, Tyler RS, Woodworth GG, Tye-Murray N, Fryauf-Bert-schy H. Results of multichannel cochlear implants in congenital and acquired prelingual deafness in children: five-year follow-up. Am J Otol. 1994; 15:1–7. [PubMed: 8572105]

Gulley RL, Landis DM, Reese TS. Internal organization of membranes at endbulbs of Held in the anteroventral cochlear nucleus. J Comp Neurol. 1978; 180:707–741. [PubMed: 210196]

Heid S, Hartmann R, Klinke R. A model for prelingual deafness, the congenitally deaf white cat—population statistics and degenerative changes. Hear Res. 1998; 115:101–112. [PubMed: 9472739]

Hultcrantz M, Snyder R, Rebscher S, Leake P. Effects of neonatal deafening and chronic intracochlear electrical stimulation on the cochlear nucleus in cats. Hear Res. 1991; 54:272–280. [PubMed: 1938629]

Jhaveri S, Morest DK. Sequential alterations of neuronal architecture in nucleus magnocellularis of the developing chicken: a Golgi study. Neuroscience. 1982a; 7:837–853. [PubMed: 7099421]

Jhaveri S, Morest DK. Sequential alterations of neuronal architecture in nucleus magnocellularis of the developing chicken: an electron microscope study. Neuroscience. 1982b; 7:855–870. [PubMed: 7099422]

Kawano A, Hakuhisa E, Funasaka S. [Effects of chronic electrical stimulation on cochlear nuclear neuron size in deaf kittens]. Nippon Jibiinkoka Gakkai Kaih. 1996; 99:884–894.

Kawano A, Seldon HL, Clark GM, Hakuhisa E, Funasaka S. Effects of chronic electrical stimulation on cochlear nuclear neuron size in deaf kittens. Adv Otorhinolaryngol. 1997; 52:33–35. [PubMed: 9042444]

Keithley EM, Feldman ML. Spiral ganglion cell counts in age-graded series of rat cochleas. J Comp Neurol. 1979; 188:429–442. [PubMed: 489802]

Klinke R, Kral A, Heid S, Tillein J, Hartmann R. Recruitment of the auditory cortex in congenitally deaf cats by long-term cochlear electrostimulation. Science. 1999; 285:1729–1733. [PubMed: 10481008]

Klinke R, Hartman R, Heid S, Tillein J, Kral A. Plastic changes in the auditory cortex of congenitally deaf cats following cochlear implantation. Audiol Neurootol. 2001; 6:203–206. [PubMed: 11694728]

Konishi M. Birdsong: from behavior to neuron. Annu Rev Neurosci. 1985; 8:125–170. [PubMed: 3885827]

Kral A, Hartmann R, Tillein J, Heid S, Klinke R. Delayed maturation and sensitive periods in the auditory cortex. Audiol Neurootol. 2001; 6:346–362. [PubMed: 11847463]

Kral A, Hartmann R, Tillein J, Heid S, Klinke R. Hearing after congenital deafness: central auditory plasticity and sensory deprivation. Cereb Cortex. 2002; 8:797–807. [PubMed: 12122028]

Kral A, Tillein J, Heid S, Klinke R, Hartmann R. Cochlear implants: cortical plasticity in congenital deprivation. Prog Brain Res. 2006; 157:283–313. [PubMed: 17167917]

Kretzmer EA, Meltzer NE, Haenggeli CA, Ryugo DK. An animal model for cochlear implants. Arch Otolaryngol Head Neck Surg. 2004; 130:499–508. [PubMed: 15148168]

Leake PA, Hradek GT. Cochlear pathology of long term induced deafness in cats. Hear Res. 1988; 33:11–33. [PubMed: 3372368]

Leake PA, Hradek GT, Snyder RL. Chronic electrical stimulation by a cochlear implant promotes survival of spiral ganglion neurons after neonatal deafness. J Comp Neurol. 1999; 412:543–562. [PubMed: 10464355]

Leake PA, Hradek GT, Vollmer M, Rebscher SJ. Neurotrophic effects of GM1 ganglioside and electrical stimulation on cochlear spiral ganglion neurons in cats deafened as neonates. J Comp Neurol. 2007; 501:837–853. [PubMed: 17311311]

Lee DJ, Cahill HB, Ryugo DK. Effects of congenital deafness in the cochlear nuclei of Shaker-2 mice: an ultra-structural analysis of synapse morphology in the endbulbs of Held. J Neurocytol. 2003; 32:229–243. [PubMed: 14724386]

Lenn NJ, Reese TS. The fine structure of nerve endings in the nucleus of the trapezoid body and the ventral coch-lear nucleus. Am J Anat. 1966; 118:375–389. [PubMed: 5917192]

Liberman MC. The cochlear frequency map for the cat: labeling auditory-nerve fibers of known characteristic frequency. J Acoust Soc Am. 1982; 72:1441–1449. [PubMed: 7175031]

Liberman MC, Brown MC. Physiology and anatomy of single olivocochlear neurons in the cat. Hear Res. 1986; 24:17–36. [PubMed: 3759672]

Limb CJ, Ryugo DK. Development of primary axosomatic endings in the anteroventral cochlear nucleus of mice. J Assoc Res Otolaryngol. 2000; 1:103–119. [PubMed: 11545139]

Lorenz K. Der Kumpan in der Umwelt des Vogels. Der Artgenosse als auslosendes Moment sozialer Verhaltensweisen. J Ornithol. 1935; 83:137–215. 289–413.

Lustig LR, Leake PA, Snyder RL, Rebscher SJ. Changes in the cat cochlear nucleus following neonatal deafening and chronic intracochlear electrical stimulation. Hear Res. 1994; 74:29–37. [PubMed: 8040097]

Mair IW. Hereditary deafness in the white cat. Acta Otolaryngol Suppl. 1973; 314:1–48. [PubMed: 4363431]

Molnar CE, Pfeiffer RR. Interpretation of spontaneous discharge patterns of neurons in the cochlear nucleus. Proc IEEE. 1968; 56:993–1004.

Moore DR, Kitzes LM. Projections from the cochlear nucleus to the inferior colliculus in normal and neonatally cochlea-ablated gerbils. J Comp Neurol. 1985; 240:180–195. [PubMed: 4056109]

Murthy VN, Schikorski T, Stevens CF, Zhu Y. Inactivity produces increases in neurotransmitter release and synapse size. Neuron. 2001; 32:673–682. [PubMed: 11719207]

Nadol JB Jr, Eddington DK. Histopathology of the inner ear relevant to cochlear implantation. Adv Otorhinolaryngol. 2006; 64:31–49. [PubMed: 16891835]

Neises GR, Mattox DE, Gulley RL. The maturation of the end bulb of Held in the rat anteroventral cochlear nucleus. Anat Rec. 1982; 204:271–279. [PubMed: 7158831]

Ni D, Seldon HL, Shepherd RK, Clark GM. Effect of chronic electrical stimulation on cochlear nucleus neuron size in normal hearing kittens. Acta Otolaryngol. 1993; 113:489–497. [PubMed: 8379304]

Nordeen KW, Killackey HP, Kitzes LM. Ascending projections to the inferior colliculus following unilateral coch-lear ablation in the neonatal gerbil, Meriones unguiculatus. J Comp Neurol. 1983; 214:144–153. [PubMed: 6841682]

Oleskevich S, Walmsley B. Synaptic transmission in the auditory brainstem of normal and congenitally deaf mice. J Physiol. 2002; 540:447–455. [PubMed: 11956335]

Oleskevich S, Youssoufian M, Walmsley B. Presynaptic plasticity at two giant auditory synapses in normal and deaf mice. J Physiol. 2004; 560:709–719. [PubMed: 15331689]

Osen KK. Cytoarchitecture of the cochlear nuclei in the cat. J Comp Neurol. 1969; 136:453–484. [PubMed: 5801446]

Pfeiffer RR. Anteroventral cochlear nucleus: wave forms of extracellularly recorded spike potentials. Science. 1966; 154:667–668. [PubMed: 5923782]

Powell TPS, Erulkar SD. Transneuronal cell degeneration in the auditory relay nuclei of the cat. J Anat. 1962; 96:249–268. [PubMed: 14488390]

Qin L, Marrs GS, McKim R, Dailey M. Hippocampal mossy fibers induce assembly and clustering of PSD95-containing postsynaptic densities independent of gluta-mate receptor activation. J Comp Neurol. 2001; 440:284–298. [PubMed: 11745624]

Quittner AL, Steck JT. Predictors of cochlear implant use in children. Am J Otol. 1991; 12(suppl):89–94. [PubMed: 2069196]

Redd EE, Pongstaporn T, Ryugo DK. The effects of congenital deafness on auditory nerve synapses and globular bushy cells in cats. Hear Res. 2000; 147:160–174. [PubMed: 10962182]

Redd EE, Cahill HB, Pongstaporn T, Ryugo DK. The effects of congenital deafness on auditory nerve synapses: type I and type II multipolar cells in the anteroventral coch-lear nucleus of cats. J Assoc Res Otolaryngol. 2002; 3:403–417. [PubMed: 12486596]

Rees S, Galdner FH, Aitkin L. Activity dependent plasticity of postsynaptic density structure in the ventral coch-lear nucleus of the rat. Brain Res. 1985; 325:370–374. [PubMed: 2983832]

Romand R, Romand MR. Myelination kinetics of spiral ganglion cells in kitten. J Comp Neurol. 1982; 204:1–5. [PubMed: 7056884]

Rubel EW, Fritzsch B. Auditory system: primary auditory neurons and their targets. Annu Rev Neurosci. 2002; 25:51–101. [PubMed: 12052904]

Rubel EW, Lippe WR, Ryals BM. Development of the place principle. Ann Otol Rhinol Laryngol. 1984; 93:609–615. [PubMed: 6508133]

Ryugo DK, Fekete DM. Morphology of primary axosomatic endings in the anteroventral cochlear nucleus of the cat: a study of the endbulbs of Held. J Comp Neurol. 1982; 210:239–227. [PubMed: 7142440]

Ryugo DK, May SK. The projections of intracellularly labeled auditory nerve fibers to the dorsal cochlear nucleus of cats. J Comp Neurol. 1993; 329:20–35. [PubMed: 8454724]

Ryugo DK, Sento S. Synaptic connections of the auditory nerve in cats: relationship between endbulbs of Held and spherical bushy cells. J Comp Neurol. 1991; 305:35–48. [PubMed: 2033123]

Ryugo DK, Wu MM, Pongstaporn T. Activity-related features of synapse morphology: a study of endbulbs of Held. J Comp Neurol. 1996; 365:141–158. [PubMed: 8821447]

Ryugo DK, Pongstaporn T, Huchton DM, Niparko JK. Ultrastructural analysis of primary endings in deaf white cats: morphologic alterations in endbulbs of Held. J Comp Neurol. 1997; 385:230–244. [PubMed: 9268125]

Ryugo DK, Rosenbaum BT, Kim PJ, Niparko JK, Saada AA. Single unit recordings in the auditory nerve of congenitally deaf white cats: morphological correlates in the cochlea and cochlear nucleus. J Comp Neurol. 1998; 397:532–548. [PubMed: 9699914]

Ryugo DK, Cahill HB, Rose LS, Rosenbaum BT, Schroeder ME, Wright AL. Separate forms of pathology in the cochlea of congenitally deaf white cats. Hear Res. 2003; 181:73–84. [PubMed: 12855365]

Ryugo DK, Kretzmer EA, Niparko JK. Restoration of auditory nerve synapses in cats by cochlear implants. Science. 2005; 310:1490–1492. [PubMed: 16322457]

Ryugo DK, Montey KL, Wright AL, Bennett ML, Pongstaporn T. Postnatal development of a large auditory nerve terminal: the endbulb of Held in cats. Hear Res. 2006:216–217. 100–115. [PubMed: 16597491]

Shapiro, WH. Device programming.. In: Waltzman, SB.; Roland, JT., Jr, editors. Cochlear implants. 2nd ed.. Thieme Medical Publishers; New York: 2006. p. 122-145.

Sharma A, Dorman MF, Spahr AJ. A sensitive period for the development of the central auditory system in children with cochlear implants: implications for age of implantation. Ear Hear. 2002; 23:532–539. [PubMed: 12476090]

Snik AF, Makhdoum MJ, Vermeulen AM, Brokx JP, van den Broek P. The relation between age at the time of cochlear implantation and long-term speech perception abilities in congenitally deaf subjects. Int J Pediatr Otorhinolaryngol. 1997; 41:121–131. [PubMed: 9306169]

Snyder WE, Pritz ME, Smith RR. Suboccipital resection of a medial acoustic neuroma with hearing preservation. Surg Neurol. 1999; 51:548–552. [PubMed: 10321887]

Stakhovskaya O, Hradek GT, Snyder RL, Leake PA. Effects of age at onset of deafness and electrical stimulation on the developing cochlear nucleus in cats. Hear Res. 2008; 243:69–77. [PubMed: 18590947]

Trune DR. Influence of neonatal cochlear removal on the development of mouse: I. Number, size and density of its neurons. J Comp Neurol. 1982; 2094:409–424. [PubMed: 7130465]

Turrigiano GG, Nelson SB. Homeostatic plasticity in the developing nervous system. Nat Rev Neurosci. 2004; 5:97–107. [PubMed: 14735113]

Tyler RS, Summerfield AQ. Cochlear implantation: relationships with research on auditory deprivation and acclimatization. Ear Hear. 1996; 17:38S–50S. [PubMed: 8807275]

Vale C, Sanes DH. The effect of bilateral deafness on excitatory and inhibitory synaptic strength in the inferior colliculus. Eur J Neurosci. 2002; 16:2394–2404. [PubMed: 12492434]

Van der Loos H, Woolsey TA. Somatosensory cortex: structural alterations following early injury to sense organs. Science. 1973; 179:395–398. [PubMed: 4682966]

Vollmer M, Leake PA, Beitel RE, Rebscher SJ, Snyder RL. Degradation of temporal resolution in the auditory midbrain after prolonged deafness is reversed by electrical stimulation of the cochlea. J Neurophysiol. 2005; 93:3339–3355. [PubMed: 15659529]

Walsh EJ, McGee J. Postnatal development of auditory nerve and cochlear nucleus neuronal responses in kittens. Hear Res. 1987; 28:97–116. [PubMed: 3610862]

Waltzman SB, Cohen NL, Shapiro WH. The benefits of cochlear implantation in the geriatric population. Otolaryngol Head Neck Surg. 1993; 108:329–333. [PubMed: 8483603]

Waltzman SB, Cohen NL, Gomolin RH, Shapiro WH, Ozdamar SR, Hoffman RA. Long-term results of early cochlear implantation in congenitally and prelingually deafened children. Am J Otol. 1994; 15(Suppl 2):9–13. [PubMed: 8572107]

Waltzman SB, Cohen NL, Gomolin RH, Green JE, Shapiro WH, Hoffman RA, Roland JT Jr. Open-set speech perception in congenitally deaf children using cochlear implants. Am J Otol. 1997; 18:342–349. [PubMed: 9149829]

Wang Y, Manis PB. Synaptic transmission at the coch-lear nucleus endbulb synapse during age-related hearing loss in mice. J Neurophysiol. 2005; 94:1814–1824. [PubMed: 15901757]

Weller WL, Johnson JI. Barrels in cerebral cortex altered by receptor disruption in newborn, but not in five-day-old mice (Cricetidoe and Muridae). Brain Res. 1975; 83:504–508. [PubMed: 1111817]

Wenthold RJ. Evidence for a glycinergic pathway connecting the two cochlear nuclei: an immunocytochemical and retrograde transport study. Brain Res. 1987; 415:183–187. [PubMed: 3304530]

West CD, Harrison JM. Transneuronal cell atrophy in the congenitally deaf white cat. J Comp Neurol. 1973; 151:377–378. [PubMed: 4754840]

Whiting B, Moiseff A, Rubio ME. Cochlear nucleus neurons redistribute synaptic AMPA and glycine receptors in response to monaural conductive hearing loss. Neurosci. 2009; 163:1264–1276.

Wilson BS, Finley CC, Lawson DT, Wolford RD, Eddington DK, Rabinowitz WM. Better speech recognition with cochlear implants. Nature. 1991; 352:236–238. [PubMed: 1857418]

Winer JA. Decoding the auditory corticofugal systems. Hear Res 207 Review. Corrected and published in Hear Res. 2006; 212:1–8.

Yasui T, Fujisawa S, Tsukamoto M, Matsuki N, Ikegaya Y. Dynamic synapses as archives of synaptic history: state-dependent redistribution of synaptic efficacy in the rat hippocampal CA1. J Physiol. 2005; 566:143–160. [PubMed: 15845579]

Zenisek D, Steyer JA, Almers W. Transport, capture and exocytosis of single synaptic vesicles at active zones. Nature. 2000; 406:849–854. [PubMed: 10972279]

Zhang LI, Bao S, Merzenich MM. Disruption of primary auditory cortex by synchronous auditory inputs during a critical period. Proc Natl Acad Sci U S A. 2002; 99:2309–2314. [PubMed: 11842227]

Zhou X, Nagarajan N, Mossop BJ, Merzenich MM. Influences of un-modulated acoustic inputs on functional maturation and critical-period plasticity of the primary auditory cortex. Neuroscience. 2008; 154:390–396. [PubMed: 18304741]

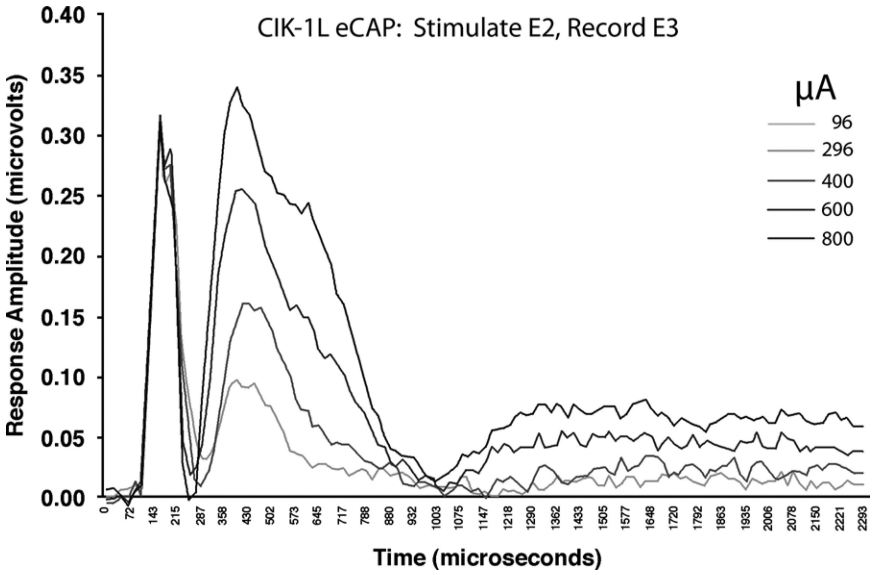

Figure 1.

Representative eCAP (electrically evoked compound action potential) collected from the ipsilateral auditory nerve of cat CIK-1 implanted at 3 months of age. Electrical stimulation was delivered to the cochlea by electrode 2, and the nerve response was recorded by electrode 3.

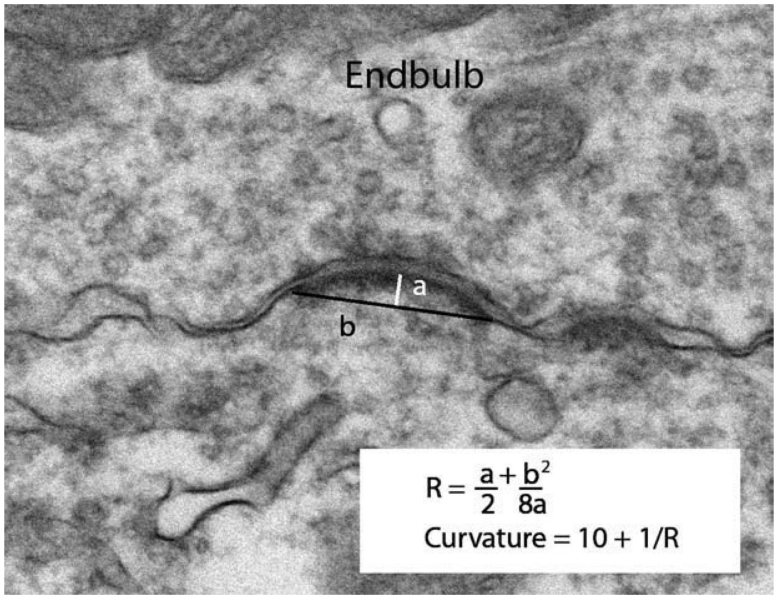

Figure 2.
Diagram illustrates method used to calculate PSD curvature. The radius of curvature (R) of the postsynaptic thickening is determined by using the chord perpendicular (a) and chord length (b).

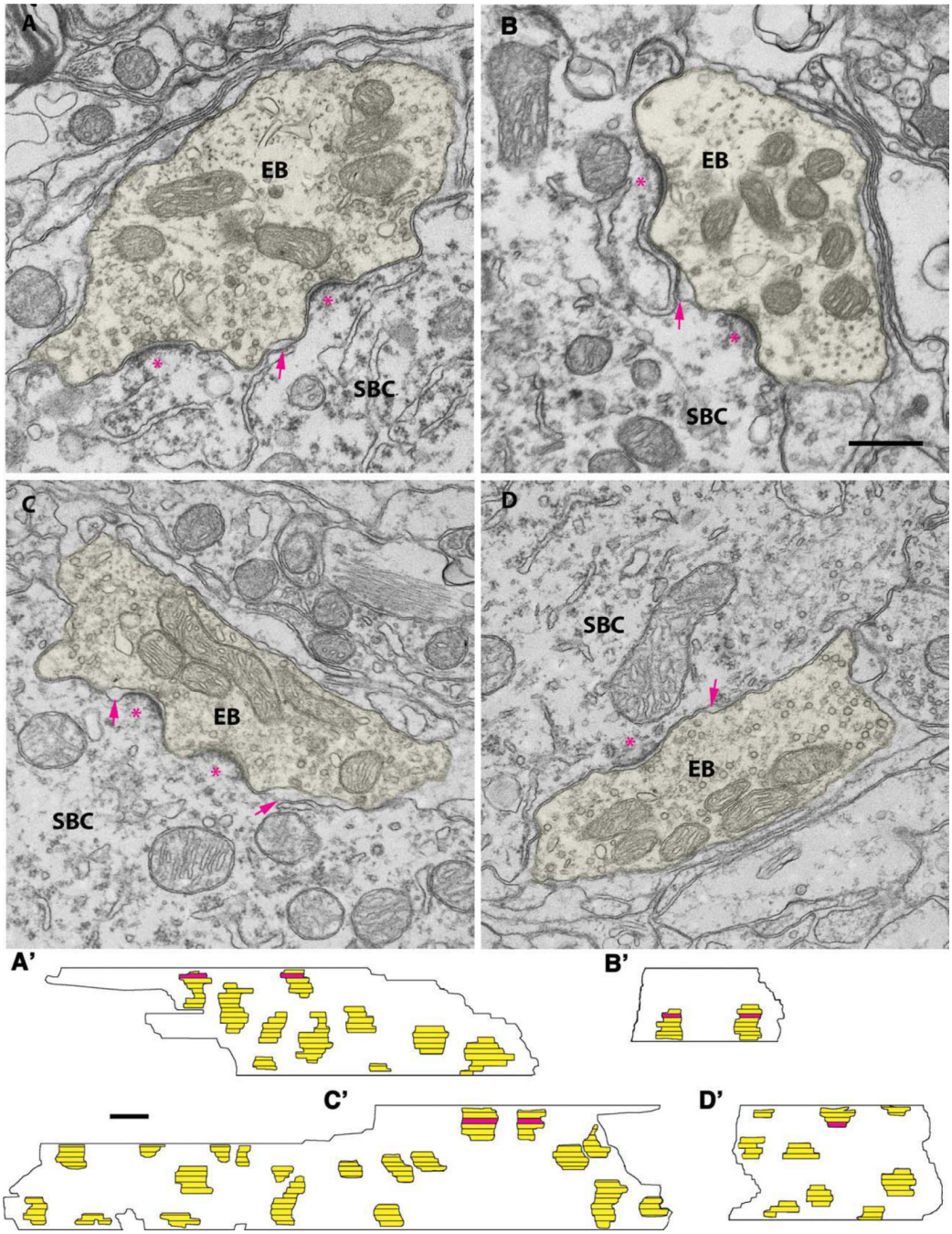

Figure 3.

A–**D**: Electron micrographs of endbulbs of Held (EB; highlighted in yellow) from normal hearing cats. The micrographs show the typical dome-shaped appearance of PSDs (*) and associated synaptic vesicles. **A′**–**D′**: The drawings display corresponding en face views of the 3-D reconstructions of PSDs, illustrating the surface of the spherical bushy cell (SBC) that lies beneath the endbulb. Each PSD from serial sections (A′,B′) is shown (yellow), and horizontal lines indicate section edges. The red area highlights the section of the EB series shown in the electron micrographs. Arrows indicate cisternae. Scale bar = 0.5 μm in B (applies to A–D) and C′ (applies to A′–D′).

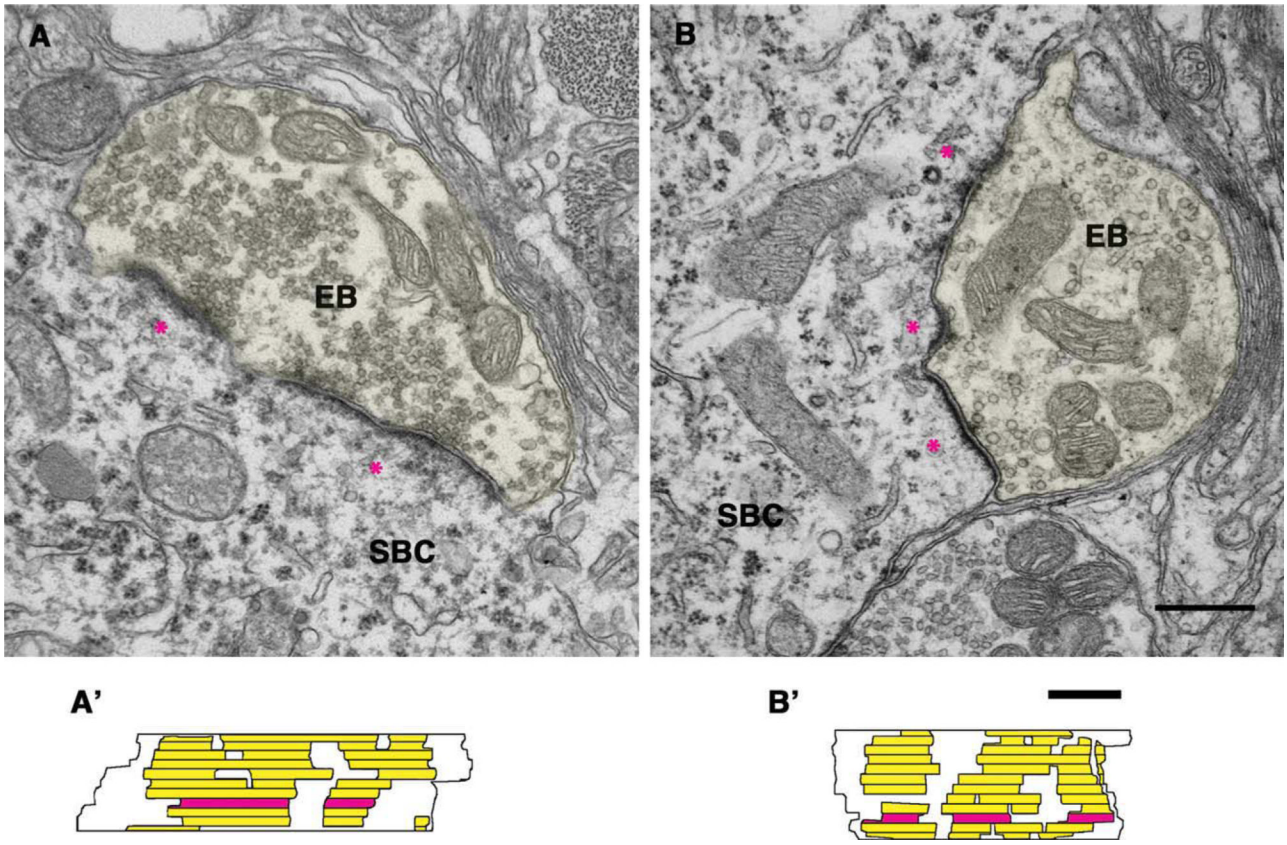

Figure 4.

A,B: Electron micrographs of endbulb of Held (EB) profiles (yellow) from congenitally deaf cats. These endbulbs display the abnormally long and flattened PSDs (*) and increased clustering of associated synaptic vesicles. **A′**,**B′**: The 3-D reconstructions of PSDs illustrate the hypertrophy of the PSDs (yellow). The horizontal lines mark the section edges, and the red strip highlights the section of the EB series shown in the above micrographs. SBC, spherical bushy cell. Scale bar = 0.5 μm in B (applies to A,B) and B′ (applies to A′,B′).

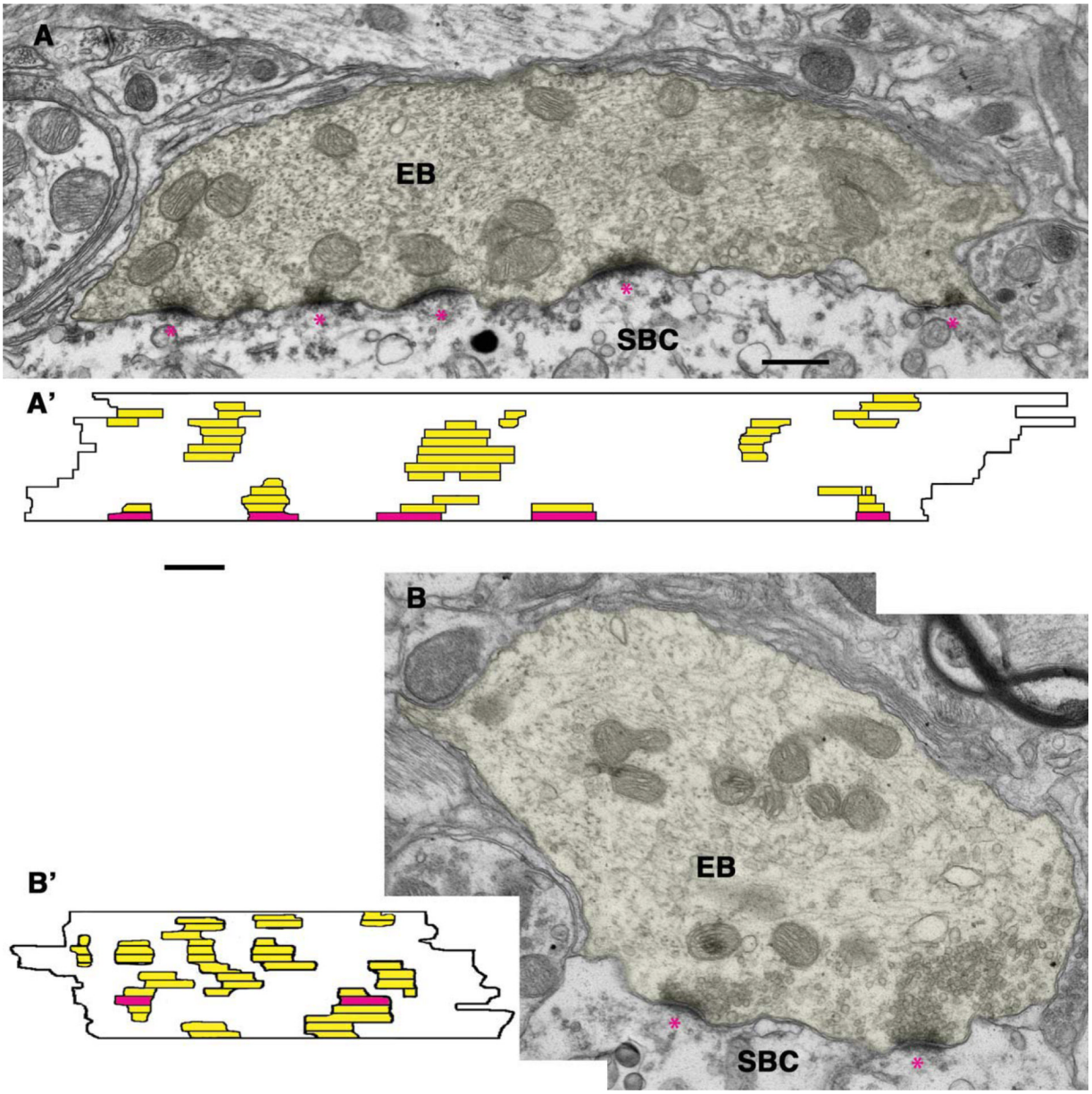

Figure 5.

A,B: Electron micrographs of endbulb of Held (EB) profiles (yellow) ipsilateral to the cochlear implant placed in 3-month-old congenitally deaf cats. Note that the PSDs (*) are restored to their normal dome shape. **A′**,**B′**: The 3-D reconstructions illustrate the return of PSDs to their normal size and distribution. The red area highlights the sections of the EB series shown in the electron micrographs, and the horizontal lines indicate section edges. SBC, spherical bushy cell. Scale bar = 0.5 μm in A (applies to A,B) and A′ (applies to A′,B′).

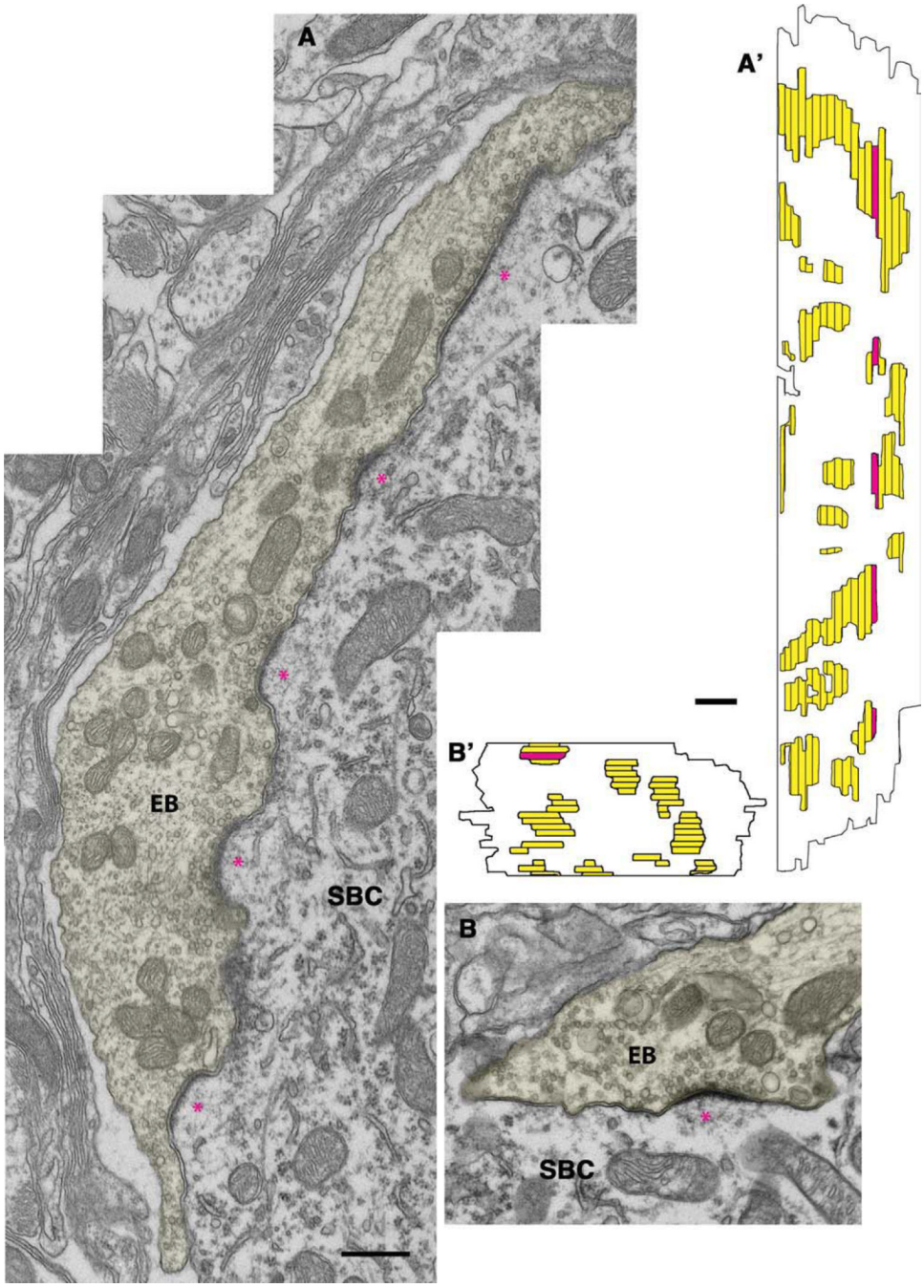

Figure 6.

A,B: Electron micrographs of endbulb of Held (EB) profiles (yellow) contralateral to the cochlear implant placed in 3-month-old congenitally deaf cats. The micrographs are representative of these animals in which the PSDs (*) are partially restored toward their normal appearance. **A′**,**B′**: The reconstructed endings illustrate that some of the PSDs are similar to those of congenitally deaf cats without implants, some appear normal, and others are intermediary between those of normal and deaf. The red areas indicate sections of the EB series that are shown in the electron micrographs, and the horizontal lines indicate section edges. SBC, spherical bushy cell. Scale bar = 0.5 μm in A (applies to A,B) and A′ (applies to A′,B′).

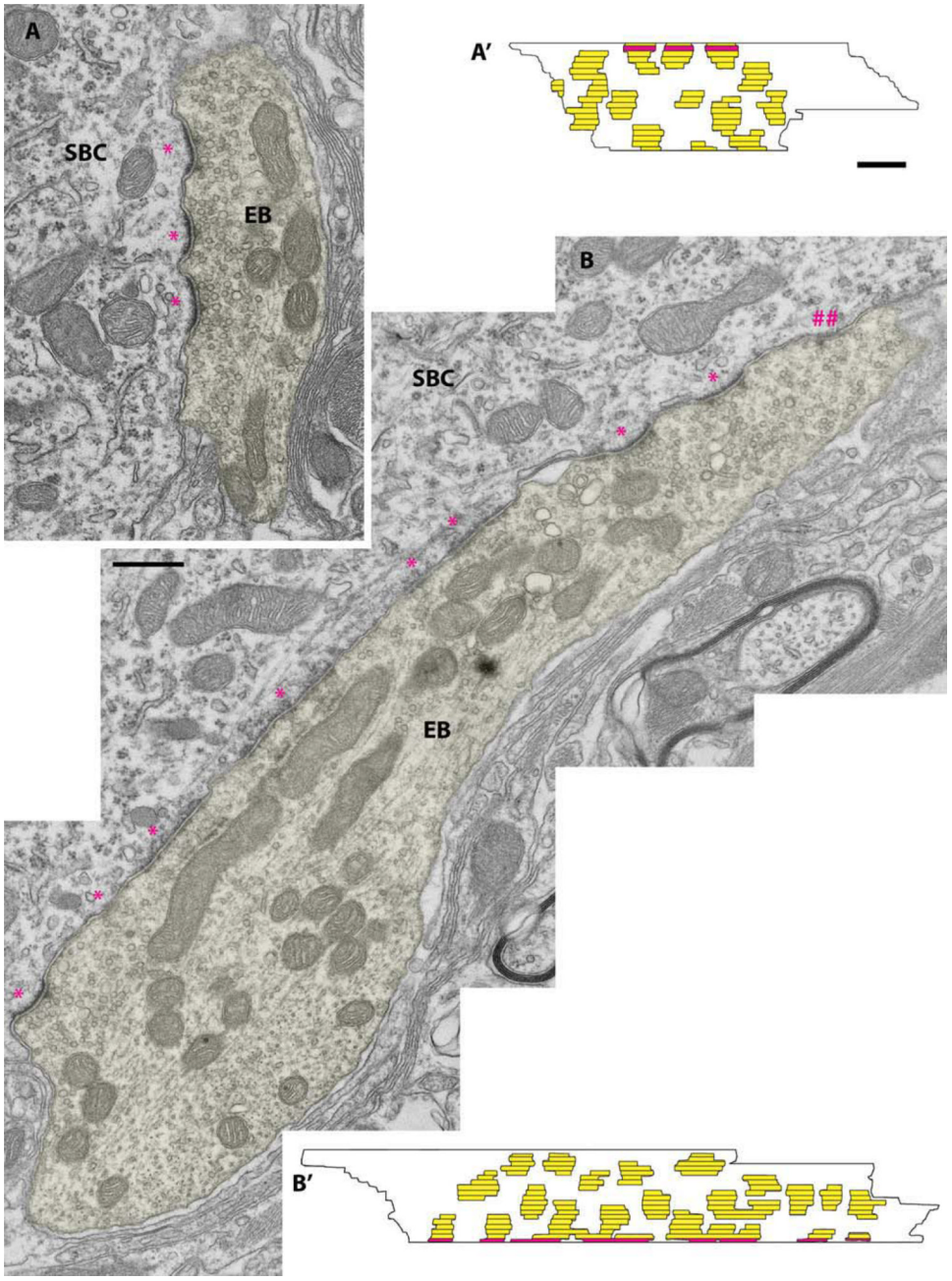

Figure 7.

A,B: Electron micrographs of endbulb of Held (EB) profiles (yellow) ipsilateral to the cochlear implant placed in 6-month-old congenitally deaf cats; (##) indicates a PSD that was present in (B) profile but was not reconstructed because it appeared in only one section. These micrographs show that the PSDs (*) in these late implanted cats have the same structural abnormalities as those in congenitally deaf cats. **A′**,**B′**: The 3-D reconstructions provide support for this conclusion. The red areas indicate sections of the EB series that are shown in the electron micrographs, and the horizontal lines indicate section edges. SBC, spherical bushy cell. Scale bar = 0.5 μm in B (applies to A,B) and A′ (applies to A′,B′).

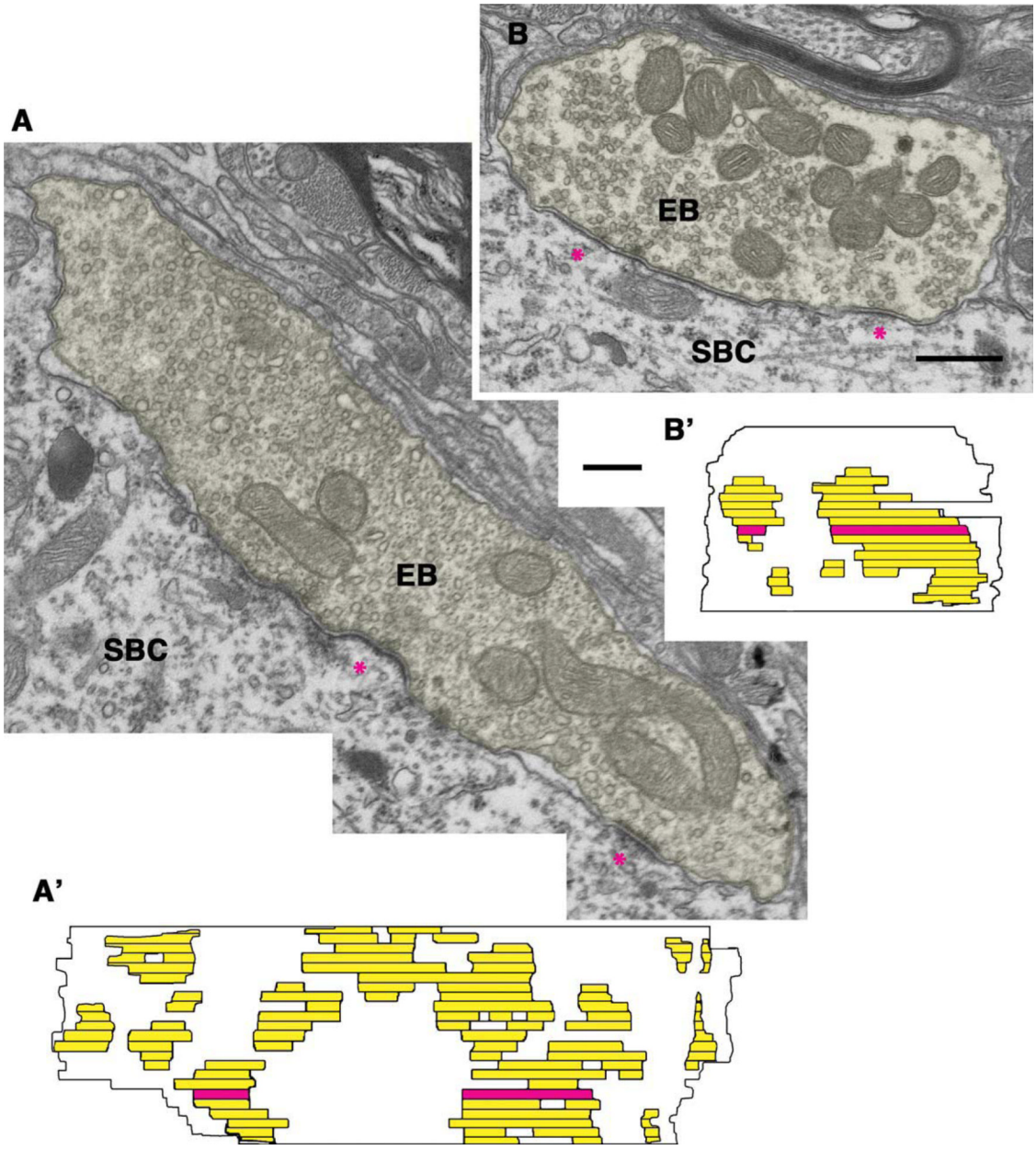

Figure 8.

A,B: Electron micrographs of endbulb of Held (EB) profiles (yellow) contralateral to the cochlear implant placed in a 6-month-old congenitally deaf cat. **A′**,**B′**: The 3-D reconstructions show that there is no effect on the PSDs from the late implanted cochlear implant. The red areas indicate sections of the EB series that are shown in the electron micrographs, and the horizontal lines indicate section edges. SBC, spherical bushy cell. Scale bar = 0.5 μm in B (applies to A,B) and B′ (applies to A′ and B′).

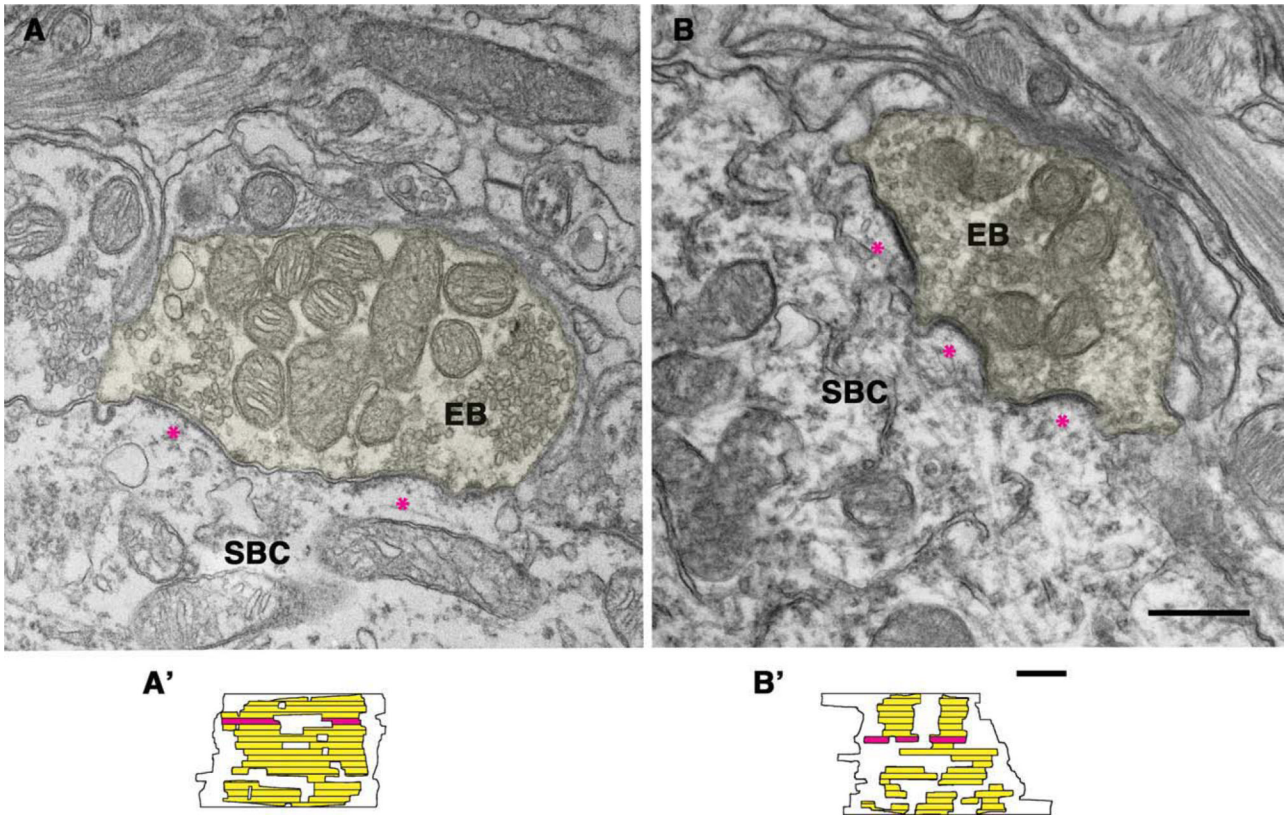

Figure 9.

A,B: Electron micrographs of endbulb of Held (EB) profiles (yellow) ipsilateral (A) and contralateral (B) to an inactivated cochlear implant placed in a 3-month old congenitally deaf cat. **A′**,**B′**: The 3-D reconstructions illustrate that cochlear implantation by itself has no effect on PSD morphology in a congenitally deaf cat. The red areas highlight the sections in the EB series in the electron micrographs. Scale bar = 0.5 μm in B (applies to A,B) and B′ (applies to A′,B′).

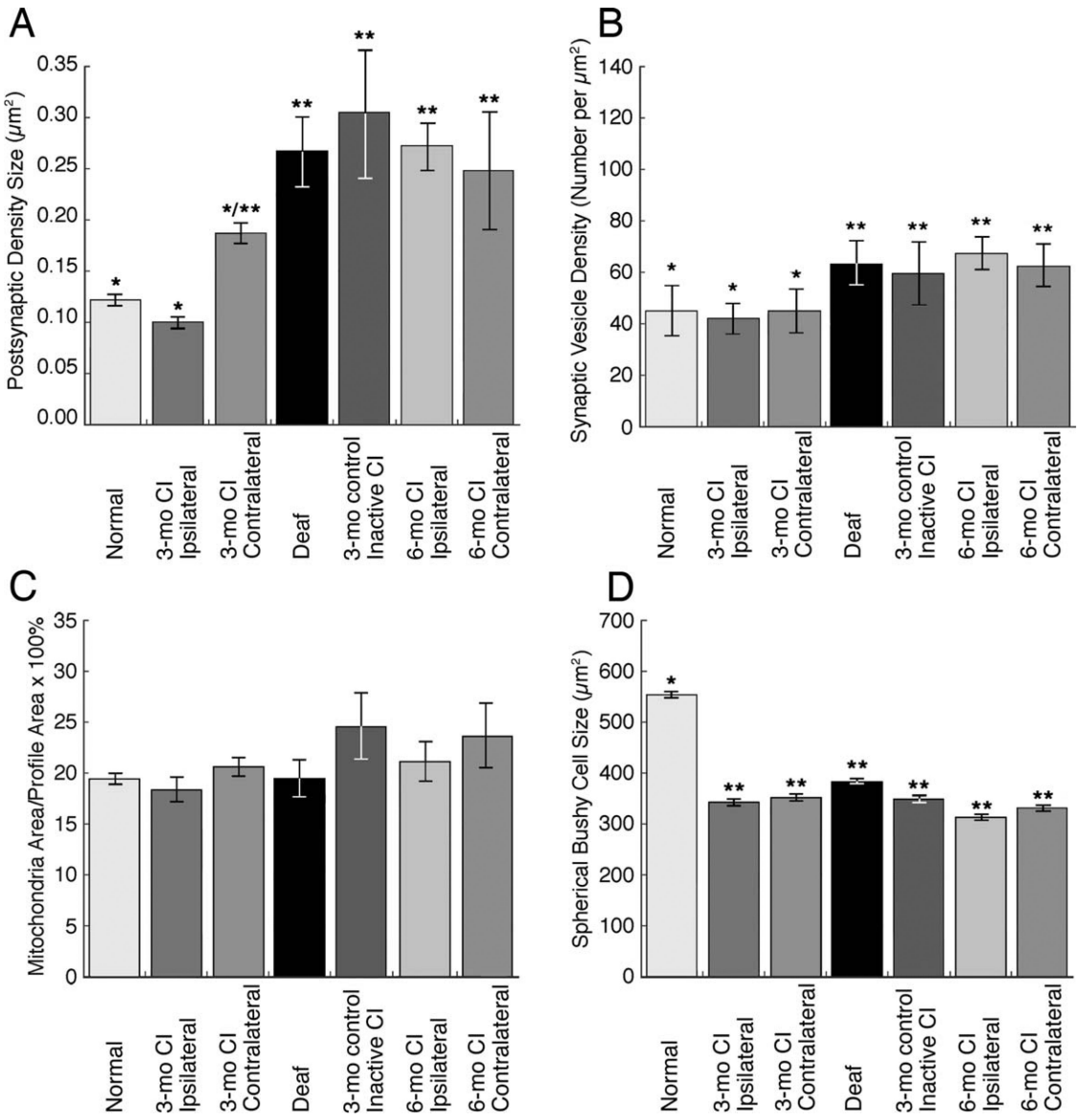

Figure 10.

Summary plots from morphometric analyses of PSD size (μm^2), synaptic vesicle density (number per μm^2), mitochondrial volume fraction (%), and spherical bushy cell size (μm^2). Number of asterisks (one or two) indicates groupings of statistical significance ($P < 0.01$ for PSD size and $P < 0.002$ for SV density, Kruskal-Wallis tests). There was no difference among the cohorts with respect to mitochondria volume fraction ($P = 0.37$, Tukey-Hanson HDS tests), and only SBCs of normal hearing cats differed in size from those of the other cohorts ($P < 0.001$, Tukey-Hanson HDS tests). The symbol (*/**) for PSD size from the 3-month-old contralateral implanted cats indicates that this group was statistically between the two groups. These plots indicate the strong effect that cochlear implants (CIs) have on the structure of synaptic endings when activated in young animals. Only ipsilateral data are shown for the inactivated control cat.

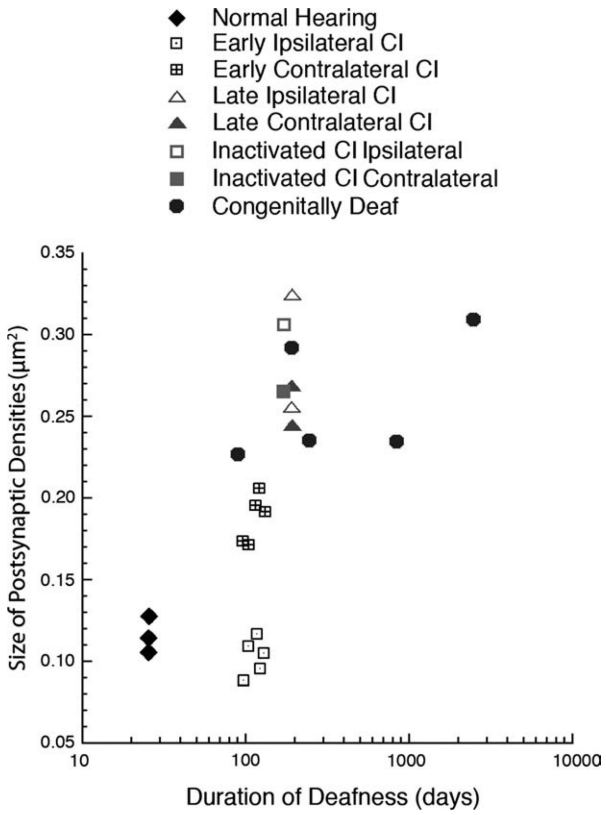

Figure 11.

Plot of average PSD size with respect to the duration of deafness. The main result is that early stimulation from a cochlear implant (CI) has a significant effect on PSD size.

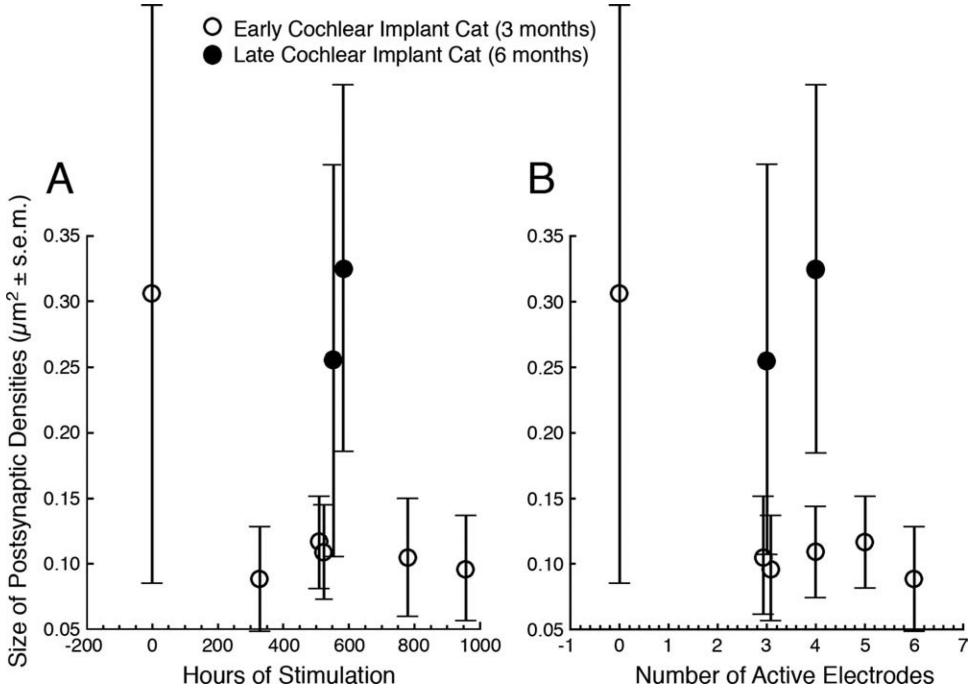

Figure 12.

A,B: Plots of average PSD size with respect to the total hours of electrical stimulation and the total number of active electrodes. For cats receiving a cochlear implant, the age at implantation is the key variable for determining the size of the PSD.

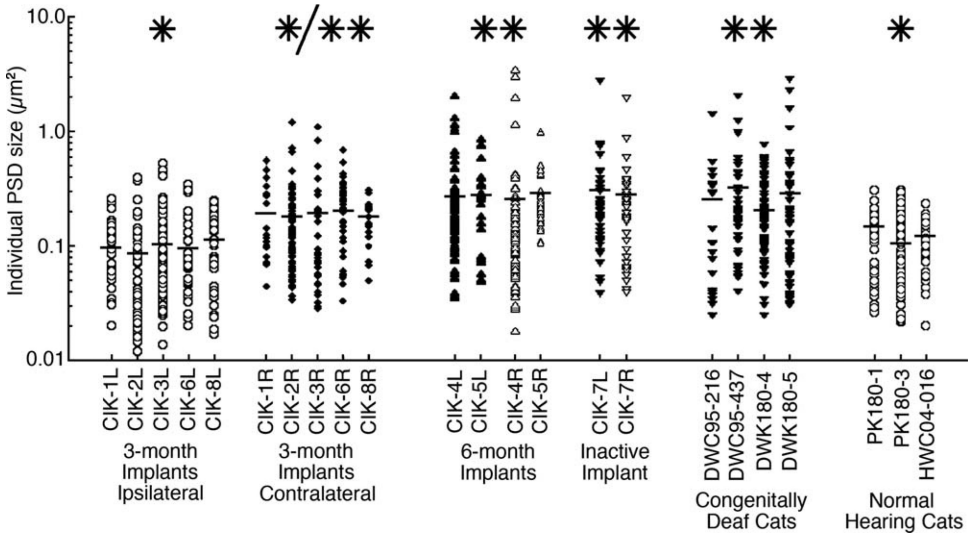

Figure 13.

Analyses of PSD size within each animal and within cohorts further show that individual animals and separate cohorts are statistically homogeneous. The single asterisk indicates cohorts that are statistically identical in value and statistically different from cohorts marked with double asterisks ($P < 0.01$). The 3-month contralateral cohort marked (*/**) is statistically indistinguishable from the other cohorts. Horizontal bars indicate cat means. On the basis of PSD size, early (3-month) implanted cats and normal hearing cats are statistically different from late (6-month) implanted cats, the inactive control cat, and congenitally deaf cats. PSDs that were subject to early but indirect contralateral stimulation were statistically determined to belong to both cohorts.

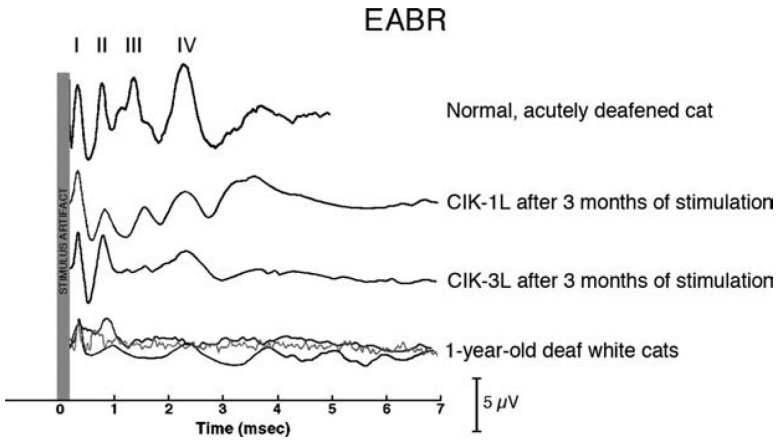

Figure 14.

Electrically evoked auditory brainstem response (eABR) recordings of cochlear-implanted, acutely deafened, and 1-year-old deaf cats. The stimulus artifact is highlighted for each recording, and peaks are denoted by Roman numerals I–IV. When peak I is aligned across recordings, it is apparent that the later peaks in unstimulated congenitally deaf cats are delayed and smaller, which is indicative of a loss of synchronous responses. In early implanted cats (CIK-1L and CIK-3L), the later peaks are more prominent but still abnormal.

TABLE 1

Subjects

Case	Implant age (days)	Activation age (days)	Termination age (days)	Amount of stimulation (hours)	No. of active leads	PSD data	SV data	SBC data
Cochlear implant cats								
CIK-1	93	116	210	510	5	x	x	x
CIK-2	75	97	165	330	6	x	x	x
CIK-3	97	128	256	781	3	x	x	x
CIK-4	173	192	284	552	3	x	x	x
CIK-5	163	193	318	584	4	x	–	x
CIK-6	90	122	296	958	3	x	x	x
CIK-8	95	105	190	522	4	x	x	x
CIK-7[1]	89	Failed	171	0	0	x	x	x
Congenitally deaf cats								
DWK180-5			191	0	–	x	x	–
DWC95-437			2,487	0	–	x	x	x
DWC95-216			835	0	–	x	x	–
DWC04-112			346	0	–	–	–	x
DWC98-338			357	0	–	–	–	x
DWK180-4			182	0	–	x	x	x
DWK90-5			90	0	–	x	–	–
Normal hearing cats								
PK180-1			182	0	–	x	–	–
PK180-2			182	0	–	–	x	–
PK180-3			185	0	–	x	–	–
04-016			180	0	–	x	x	x
97-416			179	0	–	–	–	x
98-353			1,532	0	–	–	–	x
96-259			164	0	–	–	–	x
00-087			94	0	–	–	–	x
03-026			1,896	0	–	–	x	x

Abbreviations: PSD, postsynaptic density; SV, synaptic vesicle; SBC, spherical bushy cell.

[1] Inactivated cochlear implant (CI).

TABLE 2

PSD Summary

Case	Implant age (days)	Activation age (days)	Termination age (days)	PSD size (μm^2 ± SD) Ipsilateral	PSD size (μm^2 ± SD) Contralateral
Cochlear implant cats					
Early implant					
CIK-1	93	116	210	0.117 ± 0.07	0.196 ± 0.15
				6 EBs, 41 PSDs	2 EBs, 18 PSDs
CIK-2	75	97	165	0.088 ± 0.08	0.174 ± 0.17
				6 EBs, 50 PSDs	10 EBs, 80 PSDs
CIK-3	97	128	256	0.105 ± 0.09	0.192 ± 0.23
				9 EBs, 90 PSDs	3 EBs, 35 PSDs
CIK-6	90	122	296	0.096 ± 0.08	0.206 ± 0.14
				9 EBs, 34 PSDs	9 EBs, 46 PSDs
CIK-8	95	105	190	0.109 ± 0.07	0.172 ± 0.07
				6 EBs, 37 PSDs	6 EBs, 20 PSDs
Control implant					
CIK-7[1]	89	Failed	171	0.306 ± 0.44	0.265 ± 0.32
				5 EBs, 38 PSDs	5 EBs, 37 PSDs
Late implant					
CIK-4	173	192	284	0.255 ± 0.29	0.244 ± 0.53
				14 EBs, 96 PSDs	7 EBs, 81 PSDs
CIK-5	163	193	318	0.324 ± 0.28	0.268 ± 0.17
				5 EBs, 27 PSDs	7 EBs, 29 PSDs
Congenitally deaf cats					
DWK180-5			191	0.292 ± 0.49	
				8 EBs, 66 PSDs	
DWC95-437			2487	0.309 ± 0.39	
				11 EBs, 40 PSDs	
DWC95-216			835	0.234 ± 0.31	
				7 EBs, 21 PSDs	
DWK180-4			182	0.234 ± 0.17	
				12 EBs, 83 PSDs	
DWK90-5			90	0.227 ± 0.12	
				3 EBs, 13 PSDs	
Normal hearing cats					
PK180-1			182	0.129 ± 0.08	
				12 EBs, 107 PSDs	
PK180-3			185	0.107 ± 0.05	
				3 EBs, 33 PSDs	
04-016			180	0.116 ± 0.07	
				8 EBs, 35 PSDs	

Abbreviations: PSD, postsynaptic density; EB, endbulb of Held.

[1] Inactivated cochlear implant (CI).

TABLE 3

ANOVA Values for Stimulation Parameters[1]

Source	Sum of squares	d.f.	Mean square	F	*P* value
1. Cohort	1.6991	4	0.42476	6.15	0.0001
2. Stimulation hours	0.0749	2	0.03743	0.54	0.582
3. No. of electrodes	0.1179	2	0.05897	0.85	0.4263
Error	51.6116	747	0.06909		
Total	55.7703	757			

[1]ANOVA values show that early implantation is the main variable determining PSD size.

TABLE 4

PSD Curvature (Expressed as 10 + 1/R)[1]

Cohort	Mean curvature ± SD	Grouping ($P < 0.01$)
Normal	13.895 ± 1.82	A
Early, ipsilateral implant	14.208 ± 3.49	A
Early, contralateral implant	11.273 ± 1.21	B
Late, ipsilateral implant	11.532 ± 1.57	B
Late, contralateral implant	10.002 ± 0.11	B
Inactive implant	12.239 ± 1.81	B
Deaf	11.096 ± 0.84	B

[1] Data show that synapse curvatures for normal hearing and early ipsilateral implanted cats are similar and statistically different from the less curved synapses of the other cohorts (Kruskal-Wallis tests). Cohorts indicated by different letters are significantly different.

TABLE 5

Spherical Bushy Cell (SBC) Size Data

	SBC size Ipsilateral to CI (μm^2 ± SD)		L/R difference P value
Case	**Ipsilateral to CI**	**Contralateral to CI**	**Tukey-Kramer HDS**
Cochlear implant cats			
Early implant			
CIK-1	350.2 ± 37.8	356.9 ± 44.8	No difference
	n = 111	n = 106	
CIK-2	342.3 ± 38.8	350.9 ± 45.3	<0.05
	n = 115	n = 134	
CIK-3	338.5 ± 33.8	354.7 ± 42.8	No difference
	n = 134	n = 127	
CIK-6	363.8 ± 34.3	352.8 ± 37.3	No difference
	n = 110	n = 115	
CIK-8	405.5 ± 40.1	390.6 ± 38.5	No difference
	n = 107	n = 113	
Control implant			
CIK-7[1]	327.8 ± 40.5	370.6 ± 43.5	<0.05
	n = 144	n = 134	
Late implant			
CIK-4	317.5 ± 33.7	352.6 ± 37.3	No difference
	n = 154	n = 143	
CIK-5	311.9 ± 34.1	311.3 ± 36.6	No difference
	n = 151	n = 161	
Congenitally deaf cats			
DWK180-5	392.6 ± 54.7		
	n = 48		
DWC04-112	378.3 ± 44.3		
	n = 60		
DWC98-338	381.2 ± 56.9		
	n = 119		
Normal hearing cats			
97-416	530.3 ± 82.4	558.0 ± 77.6	No difference
	n = 120	n = 50	
04-016	495.8 ± 99.5		
	n = 71		
98-353	560.3 ± 97.5		
	n = 28		
96-259	670.4 ± 81.5		
	n = 58		
00-087	427.9 ± 41.9		
	n = 29		

	SBC size Ipsilateral to CI (μm^2 ± SD)		L/R difference P value
Case	**Ipsilateral to CI**	**Contralateral to CI**	**Tukey-Kramer HDS**
03-026	589.7 ± 83.0		

[1] Inactivated cochlear implant (CI).